NATIONAL AERONAUTICS AND SPACE ADMINISTRATION

Technical Report No. 32-830

Development of the Post-Injection Propulsion System for the Mariner C Spacecraft

Bruce W. Schmitz
Thomas A. Groudle
James H. Kelley

JET PROPULSION LABORATORY
CALIFORNIA INSTITUTE OF TECHNOLOGY
PASADENA, CALIFORNIA

April 1, 1966

NATIONAL AERONAUTICS AND SPACE ADMINISTRATION

Technical Report No. 32-830

Development of the Post-Injection Propulsion System for the Mariner C Spacecraft

Bruce W. Schmitz
Thomas A. Groudle
James H. Kelley

D. Dipprey, Manager
Liquid Propulsion Section

JET PROPULSION LABORATORY
CALIFORNIA INSTITUTE OF TECHNOLOGY
PASADENA, CALIFORNIA

April 1, 1966

Prepared Under Contract No. NAS 7-100
National Aeronautics & Space Administration

CONTENTS

CONTENTS (Cont'd)

TABLES

FIGURES

ABSTRACT

This report describes the design, development, and operation of the post-injection propulsion system utilized in the *Mariner C* spacecraft. The propulsion unit consists of a small monopropellant, hydrazine-fueled rocket of 50-lbf vacuum thrust, capable of delivering a variable total impulse in conjunction with a timer-shutoff system. Functionally, the rocket is of the pressure-fed constant-thrust type. Injection pressure is obtained from a compressed gas—nitrogen—that passes through a pressure regulator and forces the propellant from a bladdered tank to the rocket engine. The rocket engine contains a quantity of catalyst to accelerate the decomposition of anhydrous hydrazine. Engine ignition is accomplished through the injection of a small quantity of a hypergolic oxidizer, nitrogen tetroxide. All valving functions for the propulsion unit are accomplished with explosively actuated valves. The propulsion system is capable of two ignitions and thrust terminations. Inflight performance of the propulsion system as a portion of the *Mariner III* and *Mariner IV* missions is described.

Author

I. INTRODUCTION

In conjunction with the *Mariner Mars* 1964 Spacecraft Development Program, a two-start, 50-lb-thrust monopropellant, hydrazine propulsion system was developed for use on the spacecraft as a trajectory-correction and maneuver rocket.

As designed for the *Mariner C* mission, this propulsion system was to remove or reduce the *Atlas-Agena* launch injection dispersion errors so that a Mars flyby with a sufficiently small miss distance could be reasonably assured. Nominally, this function was to be performed during a single spacecraft midcourse maneuver (occurring approximately 4 to 10 days after launch), at which time the spacecraft would be directed to turn to a prescribed position in space and impart a corrective impulse via the post-injection propulsion system. The second propulsion system firing was available to further refine the trajectory.

It is the purpose of this report to describe the post-injection propulsion system development program and flight history through the planetary encounter by the spacecraft.

II. SYSTEM DESCRIPTION

A. Basic Concept

The system utilizes a liquid monopropellant, anhydrous hydrazine (N_2H_4), as the propellant and develops a vacuum thrust of 50 lbf. The system is functionally a regulated gas-pressure-fed, constant-thrust rocket. The principal system components consist of a high-pressure gas reservoir, a pneumatic pressure regulator, a propellant tank and propellant bladder, an ignition reservoir, explosive valves for start and shutoff functions, and a rocket engine. The rocket engine contains a quantity of catalyst to accelerate the decomposition of the hydrazine. Ignition is accomplished by the injection of a small quantity of nitrogen tetroxide (N_2O_4). Four jet vanes are located at the exit plane of the nozzle and are used to provide spacecraft roll, yaw and pitch control during engine burn. A schematic of the system is shown in Fig. 1, and a flight-type system is depicted in Fig. 2.

The design and operational philosophy of the system was directed toward maximizing system reliability and

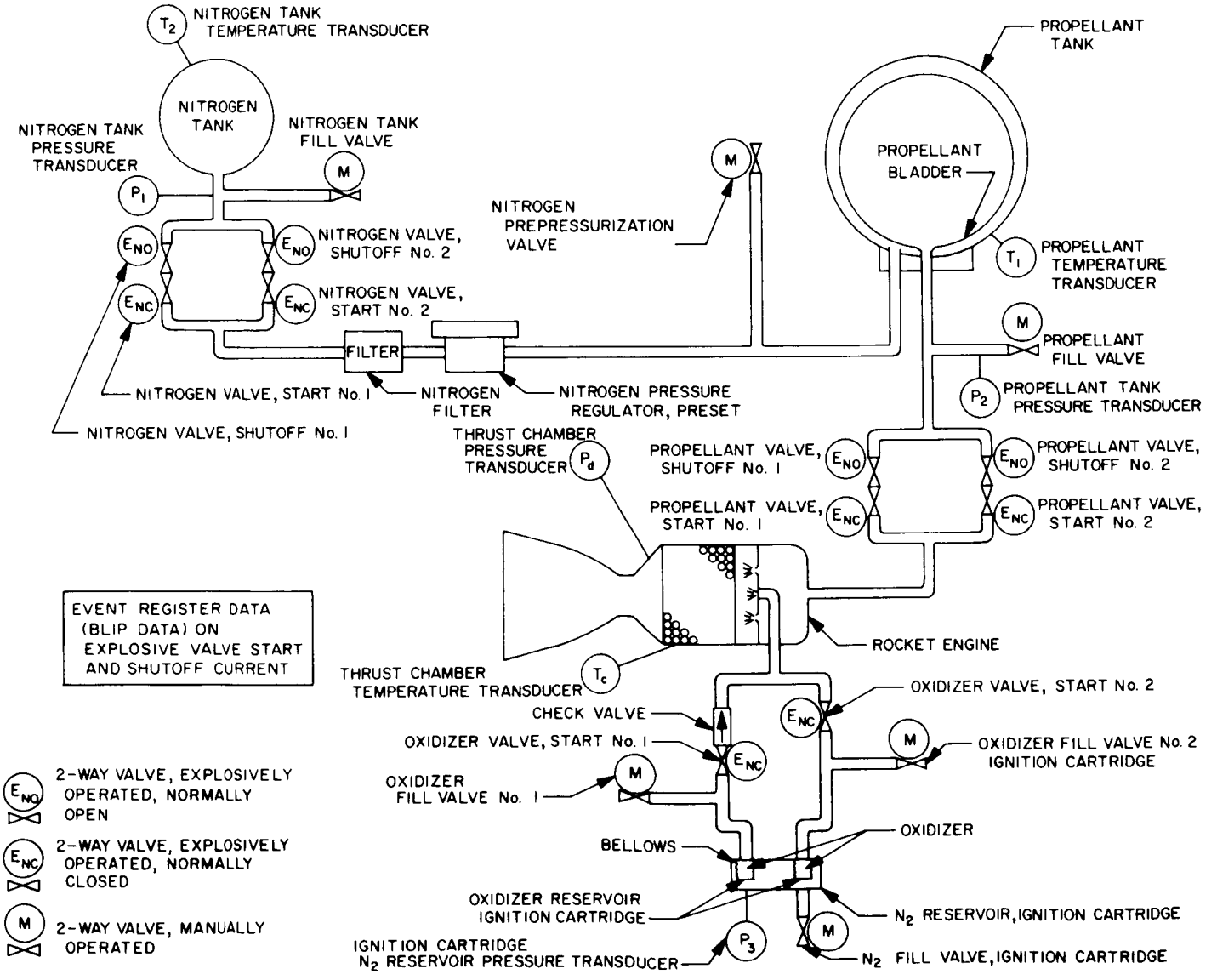

Fig. 1. *Mariner* C post-injection propulsion system schematic

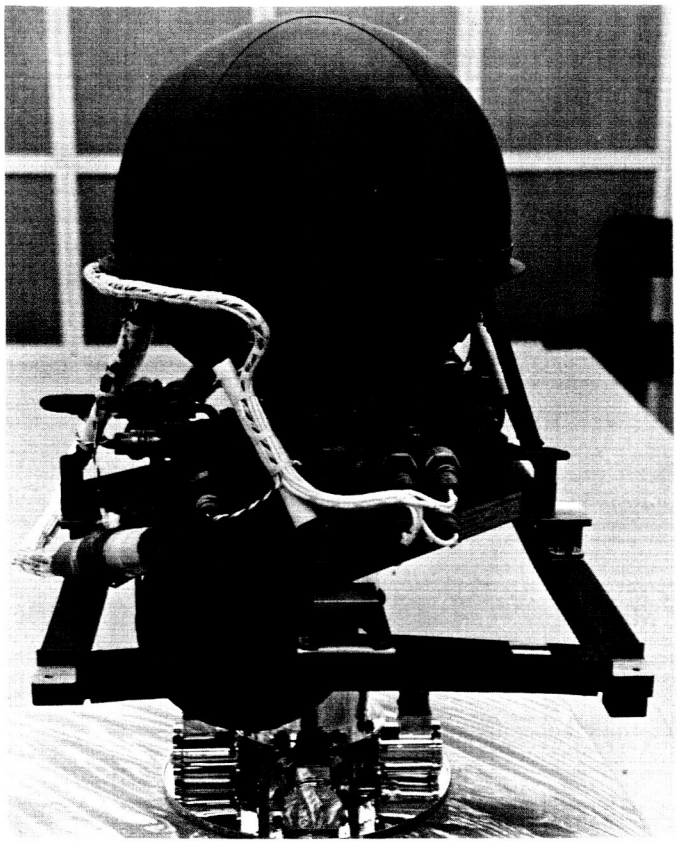

Fig. 2. Post-injection propulsion system

reproducibility, minimizing preflight handling and spacecraft interactions, minimizing inflight electrical signals and sequencing, and minimizing the number of system components.

The system concept shown in Fig. 1 was predicated on the basis that it satisfy the long-term space-storage (maximum of 250 days) and multiple start (maximum of two) requirements imposed by the *Mariner C* missions. In order to better fulfill the long-term storage requirements, pressurization by gaseous nitrogen was used in lieu of gaseous helium, the latter being more prone to leakage. In a like manner, welded and brazed tubing and fittings were used wherever possible to minimize the number of potential leak sources. Also, metal seals were used (where welding and brazing are impractical) in place of elastomeric seals to alleviate the effects of radiation, hard vacuum, and long-term storage on the critical system seals. Multiple-start capability is realized by the inclusion of *ganged* explosive valves with two parallel branches of normally closed (start)–normally open (shut-off) valve groups in the nitrogen and fuel circuits and two normally closed valves in parallel in the oxidizer circuit. Individual start cartridges (15 cc of N_2O_4 each) are used for each of the two starts, both cartridges being pressurized by a common source. Prior to actual launch, the propulsion system can be fueled, pressurized, and monitored for several weeks before its inclusion in the spacecraft. In the pressurized and fueled condition, the system is safe for personnel to work around over the temperature range of 35°F to 125°F (burst pressures of the pressure vessels = 2.2 > maximum working pressures at 125°F. No spacecraft umbilicals or hardlines are required to maintain the propulsion system in the *ready* condition. The firing of the post-injection propulsion system is controlled by the central computer and sequencer (CC&S), which receives the time, direction, and duration of the midcourse firing through the ground-to-spacecraft communication link. After the spacecraft has assumed the correct firing attitude, the post-injection propulsion system is ignited at the prescribed time through an electrical signal that is originated in the CC&S. Inasmuch as the propellant tank is prepressurized, the rocket engine ignition can occur concomitantly with the release of the high-pressure nitrogen to the regulator, without allowing time for the propellant tank pressures to build up to the normal operating level. Thrust termination is controlled by an electrical signal from the CC&S after the commanded burning time has been accomplished.

During the rocket engine firing, spacecraft attitude is maintained by the autopilot-controlled jet vanes (Fig. 3).

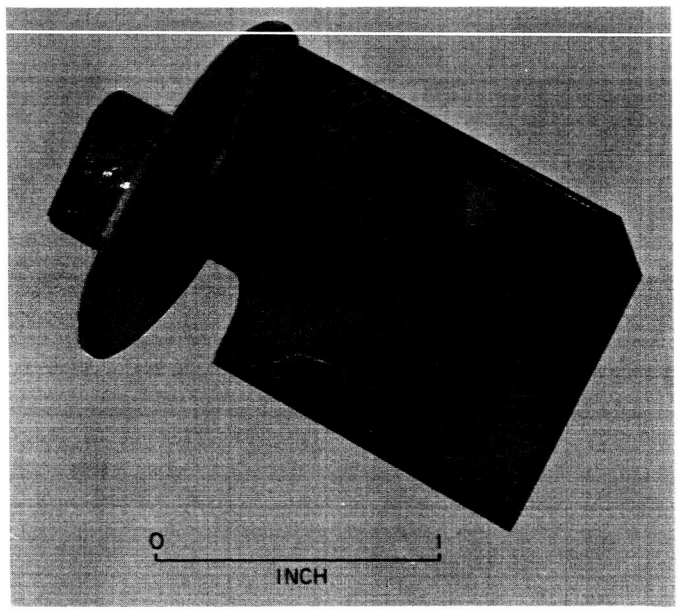

Fig. 3. Jet vane

In Fig. 1, the specific sequence of events for the propulsion system for each engine ignition and shutoff is given, as follows:

1. At the command signal from the CC&S to ignite the engine, normally closed, explosively actuated valves—nitrogen valve start No. 1 or start No. 2, propellant valve start No. 1 or start No. 2, and oxidizer valve start No. 1 or start No. 2—are activated, allowing regulated nitrogen pressurization of the propellant tank, propellant flow to the rocket engine, and injection of a small quantity of nitrogen tetroxide to the rocket engine.
2. Hypergolic ignition ensues, followed by continuous catalytic monopropellant decomposition of the anhydrous hydrazine.
3. At the command signal from the CC&S to terminate rocket thrust, normally open explosively actuated valves—propellant valve shutoff No. 1 or shutoff No. 2 and nitrogen valve shutoff No. 1 or shutoff No. 2—are activated, terminating propellant flow to the rocket engine and positively isolating the remaining pressure in the nitrogen sphere from the propellant tank.

B. Specific Design Requirements

Design requirements for the post-injection propulsion system resulted from definition of spacecraft physical and operational restraints, *Agena* injection guidance accuracies, ground and inflight environment conditions, propulsion system characteristics, and the requirements imposed in the spacecraft design characteristics and restraints.

It was determined the system should provide the following capabilities:

1. A maximum velocity increment of 60 m/sec to an 800-lb spacecraft for fulfillment of maximum expected midcourse maneuver requirements
2. A minimum midcourse correction velocity increment of 0.100 m/sec to a 600-lb spacecraft
3. Two ignitions and thrust terminations with a minimum elapsed time of 4 hr between consecutive engine firings
4. Ignition and operation in a vacuum environment
5. Ignition in a gravitationless environment
6. A preflight-to-launch ambient temperature range of 35 to 125°F
7. Temperature limits of 35 to 125°F from launch through flight termination
8. Survival of vacuum environment storage in excess of 250 days without deleterious effects on the spacecraft attitude control or performance
9. Rocket engine nominal steady-state vacuum thrust with the four jet vanes deflected through 10 deg to be $\leqq 52.5$ and $\geqq 47.5$ lbf
10. A vacuum specific impulse of 231.7 lbf-sec/lbm, corresponding, approximately, to the rocket engine vacuum thrust with all four jets vanes deflected through 10 deg
11. A variable total impulse for velocity increment requirements from 0.1 to 60 m/sec, with total impulse control by a spacecraft timer to control engine burn time, and engine total impulse and velocity increment predictable to approximately the 1σ accuracies[1] depicted in Fig. 4.
12. Thrust vector control by four jet vanes, each capable of producing 2.4 lb of lift in the fully deflected position

[1]Includes spacecraft timer errors.

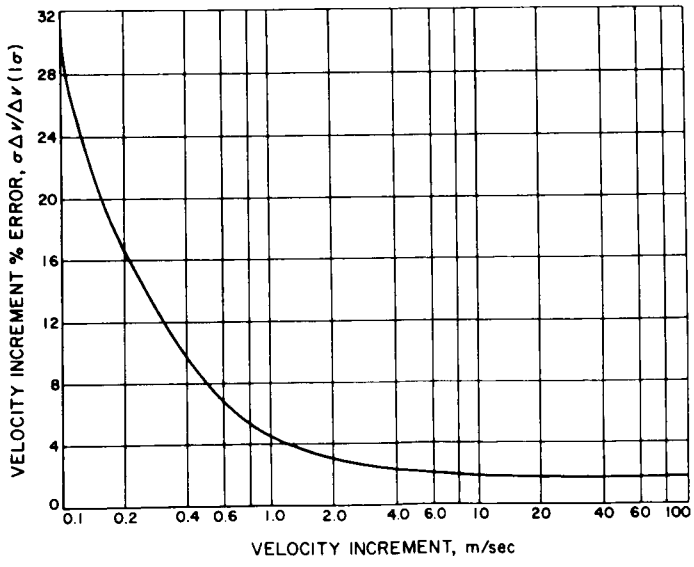

Fig. 4. Percent error (1σ) as a function of velocity increment

13. Thrust chamber and nominal thrust vector located normal to the spacecraft roll axis and coincident with the predicted spacecraft center of gravity (To permit adjusment capability of the thrust vector, the propulsion system shall be adjustable within a 1-in.-diam circle, and through the utilization of separate propulsion system-spacecraft mounting structures, the propulsion system and thrust vector shall be capable of being tilted ±2.0 deg along the spacecraft roll axis.)
14. Effective engine thrust vector predictable to within ±0.2 deg of the geometrical engine centerline measured at a plane passing through the *throat* of the engine
15. Three simultaneous dual-bridgewire squib firings for each of the two engine ignitions, and two simultaneous dual-bridgewire squib firings for each of the two engine thrust terminations with a minimum time between ignition (start) squib firings and thrust termination (shutoff) of 50 msec
16. A system which, when fueled and pressurized, is safe for personnel to work around at temperatures up to 125°F

III. PERFORMANCE CAPABILITY

The *Mariner Mars* 1964 post-injection propulsion system develops, nominally, 50 lbf of vacuum thrust at a specific impulse of 236 lbf-sec/lbm without jet vanes. Table 1 summarizes the major engine performance characteristics of the monopropellant engine and jet vane system. Length restrictions resulted in a nozzle with an expansion ratio of 44:1.[2]

Table 1. Nominal performance summary

Item	Performance value
Vacuum specific impulse (without jet vanes)[a]	236.0 $\frac{\text{lbf-sec}}{\text{lbm}}$
Vacuum specific impulse (4 jet vanes deflected 10 deg)[b]	232.7 $\frac{\text{lbf-sec}}{\text{lbm}}$
Vacuum thrust (without jet vanes)	50.71 lbf
Vacuum thrust (4 jet vanes deflected 10 deg)	50.00 lbf
Vacuum thrust coefficient[c] (without jet vanes)[a]	1.7500
Characteristic velocity[c]	4340 fps
Propellant flow rate	0.215 lbm/sec
Throat area (ambient)	0.15 in^2
Stagnation chamber pressure[c]	189 psia
Nozzle expansion ratio	44:1
Specific heat ratio	1.38
Maximum thrust vector deflection capability (2 jet vanes deflected 25 deg)	±5.0 deg

[a]Jet vane drag and lift in null position is negligible; therefore, null position engine data and engine data without jet vanes are essentially equal.
[b]Jet vane maximum deflection capability equals 25 deg, but expected maximum steady-state deflection is approximately 10 deg.
[c]Computation is based on actual steady-state hot throat area (1.99% larger than ambient temperature throat area).

Table 2 tabulates the weight breakdown of the *Mariner Mars* 1964 post-injection propulsion system. It should be noted that, as discussed in Section II, the propellant and nitrogen tanks are high-safety-factor (2.2) vessels and that the propulsion system is relatively small, with system-fixed (not affected by propellant load) weights prevailing.

Unlike the *Ranger* and *Mariner R* spacecraft, the *Mariner C* spacecraft employed a timer shutoff mechanism for the propulsion system, instead of an integrating-accelerometer circuit. The inclusion of the timer shutoff mechanism in the *Mariner C* spacecraft placed stringent total-impulse predictability and reproducibility requirements on the propulsion system. The system design was to be capable of providing a variable total impulse for fulfillment of velocity increment requirements ranging from 0.1 m/sec, for a 600-lb spacecraft, to 60 m/sec for an 800-lb spacecraft. The total impulse control was provided by the timer, which controlled the engine burn

[2]Early in the program, before the nozzle expansion ratio was fixed, an engine with an expansion ratio of 103:1 was designed, fabricated, and tested in a near-vacuum environment. This engine delivered a vacuum specific impulse of 243 lbf-sec/lbm.

Table 2. Propulsion system weight breakdown

System component breakdown	Weight, lb	System component breakdown	Weight, lb	
Propulsion structure assembly	3.87	Nitrogen tank temperature transducer	0.02	
Engine and catalyst	2.50	Oxidizer start cartridge	2.40	
Engine insulation	0.10	Tubing and fittings	3.20	
Propellant tank	2.80	Thrust vector control assembly	2.60	
Propellant bladder	1.00	Pyrotechnic harness	0.69	
Propellant valve	1.50	Instrumentation harness	0.69	
Propellant tank pressure transducer	0.27	Subtotal dry unserviced weight		26.68
Propellant tank temperature transducer	0.10	Propellant	21.50	
Oxidizer pressure transducer	0.27	Oxidizer	0.13	
Thrust chamber pressure transducer	0.30	Nitrogen gas	1.00	
Nitrogen tank	1.90	Squibs	0.62	
Nitrogen valve	1.00	Subtotal		23.25
Nitrogen pressure regulator	1.20	Total loaded weight	49.93	49.93
Nitrogen tank pressure transducer	0.27			

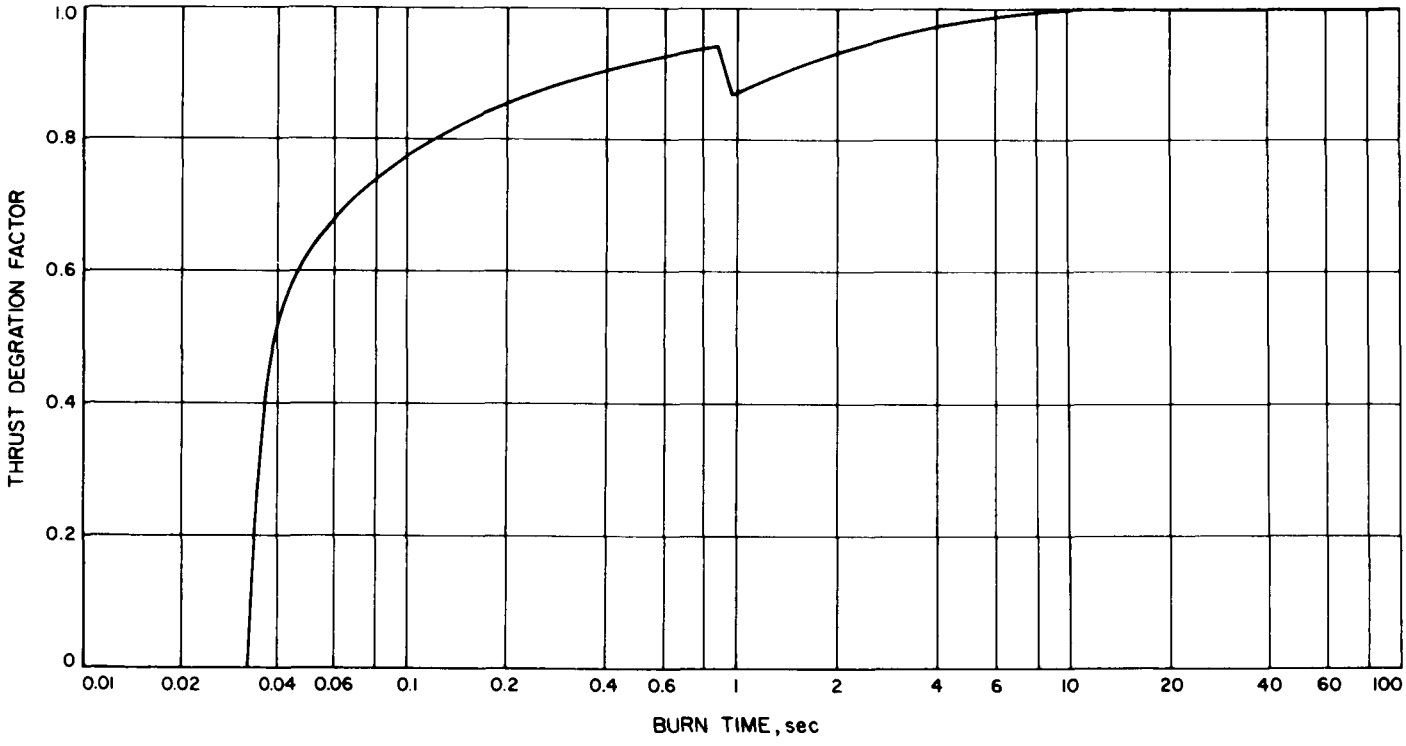

Fig. 5. Thrust degradation factor as a function of burn time

time. An error analysis indicated that the engine total impulse and velocity increment could be predictable to approximately the 1σ accuracies depicted in Fig. 4, including timer errors and resolution. Removal of the timer errors and timer resolution, as well as subsequent improvements in the propulsion system testing and instrumentation techniques, reduced these errors by a factor of 3, as discussed in Appendix A.

Typically, monopropellant hydrazine rocket engines have an ignition transient, during which the engine operates at reduced performance while the catalyst bed reaches thermal equilibrium. Because of the spacecraft mechanization for engine-burn duration (commanded fixed-burn time as compared with accelerometer shutoff), the prediction of the thrust transient was of paramount importance in minimizing correction dispersion errors. A

thrust degradation factor, which accounts for the reduced engine performance, was experimentally determined through a series of propulsion system tests; this factor is depicted as a function of time in Fig. 5. Reduction of test data showed that 0.14 lb additional propellant is needed to compensate for the start transient performance degradation; therefore, to determine the propellant needed to provide a given spacecraft with a given velocity increment, this value should be added to that obtained from the momentum exchange relationship.

The minimum velocity increment capability of the propulsion system is very important, since, statistically, an extremely small correction has a finite probability of being required to correct for injection or previous correction dispersion errors. The design goal of the *Mariner Mars* 1964 propulsion system was to be able to supply a minimum velocity increment capability of 0.1 m/sec to a 600-lb spacecraft. For velocity increments of this magnitude, the tailoff impulse from the propellant contained downstream of the shutoff valve contributes significantly to the total impulse required. Experimental and analytical programs were conducted to define the engine tailoff impulse as a function of engine burn time.

Engine tests were run for durations of 0.1, 0.3, 1.0, 5.0, 10.0, 30, 60, and 100 sec, and careful tailoff impulse measurements were made. The experimental results agreed very closely with the analytical prediction, which was later modified to more nearly fit the experimental data, resulting in a curve of engine tailoff impulse vs burn time as depicted in Fig. 6 (see also Appendix B).

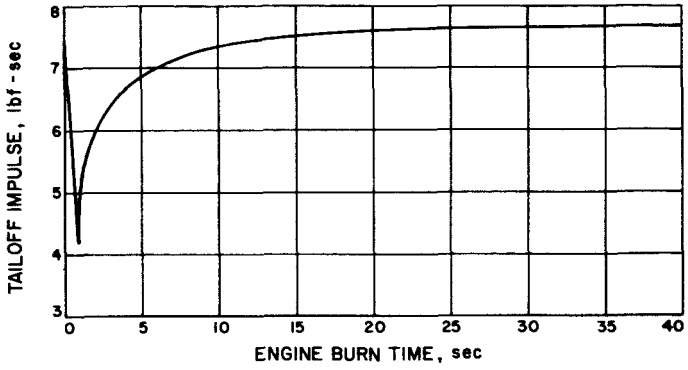

Fig. 6. Tailoff impulse as a function of engine burn time

IV. DEVELOPMENT AND TYPE-APPROVAL TEST PROGRAM

A. Design Development

The initial planning, design approach, and configuration studies were initiated in June 1962 in conjunction with the initial design studies of the 1964 Mars mission. Several approaches to the two-start and long-term space storage requirements were considered, and preliminary system designs were made of these approaches. In September 1962, the system design shown in Fig. 1 was selected as the one best satisfying the mission requirements and having a high probability of successful development. (See Table 3 for list of JPL documentation.) Utilizing a spontaneous catalyst in lieu of an oxidizer (N_2O_4) start slug system was considered as a possible modification to the design depicted in Fig. 1. Promising results in the development of a catalyst producing spontaneous decomposition of anhydrous hydrazine at ambient temperatures had been achieved.[3] In April 1963, it was decided that the catalyst had not been developed sufficiently for this application, so consideration of its use was terminated.

Since a wide spectrum of temperature environment would be applied to the spacecraft and propulsion system, it was necessary to use a special paint[4] to provide thermal control above the propulsion system mounting plate. Everything below the plate was highly polished (see Fig. 2).

[3] Work accomplished by Shell Development Company under NASA Contract NAS 7-97.

[4] Cat-a-lac Black, Finch Paint and Chemical Corp., Torrance, Calif.

Table 3. JPL documentation of post-injection propulsion system

No.	Description
	Specifications
MC-4-610	Functional Specification, *Mariner* C Flight Equipment, Postinjection Propulsion System
20009	Process Specification, Safety with Lockwire
20503	Process Specification, Torque Limits for Spacecraft Structural Fasteners RA-1 Through RA-9
30009	Process Specification, Liquid Propulsion System, Cleaning and Packaging of System Components
30209	Vega Process Specification, Flight Equipment, Titanium Alloy 6 Al 4 V Compressed GPS Vessels
30250 B	Environmental Specification, *Mariner* C Flight Equipment, Type Approval Environmental Test Procedure
30251 B	Environmental Specification, *Mariner* C Flight Equipment, Flight Acceptance Environmental Test Procedure
31192	Design Specification, *Mariner* C Flight Equipment, Explosively Actuated Valve Assemblies
31252	General Specification, *Mariner* C Flight Equipment, *Mariner* C Requirements for Minimum Magnetic Field
MCM-31525-TST	Test Specification, *Mariner* C Flight Equipment, Postinjection Propulsion System, Rocket Engine
MCM-31526-TST	Test Specification, *Mariner* C Flight Equipment, Postinjection Propulsion System, Pneumatic Regulator
MCM-31527-TST	Test Specification, *Mariner* C Flight Equipment, Postinjection Propulsion System, Oxidizer Start Cartridge
	Procedures
CM 105.00	*Mariner* C Postinjection Propulsion System, Leak Check, Propellant Fill, and Pressurization Procedure
CM 108.00	*Mariner* C Postinjection Propulsion System, Detailed Assembly Procedure
CM 217.00	*Mariner* C Spacecraft Pyrotechnics Preflight Evaluation (ETR)

Upon completion of the spacecraft preliminary design and finalization of the system schematic, a methodical development program was initiated, with the goal of delivering the first flight-acceptance (FA) tested propulsion system for incorporation into the *Mariner Mars* 1964 proof test model (PTM) in November 1963. Reference 1 describes the chronological development in detail, and Table 4 represents the propulsion system development schedule.

B. Component Type-Approval Tests

Type-approval tests conducted on seven components are described here. Figure 7 illustrates the sequence of the tests.

1. Rocket Engine

The rocket engine used in the propulsion system was essentially identical to that used in the *Ranger* propulsion system (Fig. 8). The only modifications were (1) changes in flange attachments to components for packaging purposes, (2) the addition of a chamber pressure tap for inflight telemetry of chamber pressure during engine burn, and (3) the addition of an insulation jacket around the engine chamber wall to preclude radiant heat transfer to the spacecraft during engine burn.

Two rocket engines were subjected to TA testing. One rocket engine was subjected to the environmental tests of humidity, shock, static acceleration and boost-phase vibration. These tests were followed by two engine firings at nominal chamber pressure, each of 300-sec duration. No anomalies were noted in either of the tests. A second engine was subjected to FA tests consisting of an injector performance test and a boost-phase vibration test. Upon completion of these tests, an attempt was made to fire the engine at a chamber pressure of ~ 285 psia (1.5 times nominal chamber pressure) for 300 sec. A failure of the chamber wall occurred at the end of 71-sec operating time. This test had previously been passed on the *Ranger Block III* engine, which is essentially identical in design. However, post-test analysis indicated that the previously described insulation jacket raised the wall temperature by approximately 200°F, and this temperature increase, compounded by the abnormal chamber pressure, stressed the wall material above its yield point. The chamber-wall thickness was subsequently changed from 0.031 in. to 0.045 in. The engine was then successfully fired twice at a chamber pressure of 235 psia (1.25 times nominal chamber pressure); each test was for 200 sec. Two tests, 100 sec each, were then made with the engine installed in an inverted position. The purpose of these tests was to demonstrate that propellant contained between the valve and injector will vaporize at engine shutdown without detonating, because of heat soak back from the catalyst bed. Subsequently, the engine was fired at 1.33, 1.50, and 1.67 times nominal chamber pressure, each test being 200 sec. All tests with the 0.045-in.-thick chamber were successfully completed and, thus, the engine design was considered qualified for flight.

2. Oxidizer Start Cartridge

The start cartridge used on the *Mariner C* propulsion system is similar to that used on the *Ranger Block III* propulsion system. The design was modified to provide a two-start capability as shown in Fig. 9. It consists of

Table 4. Propulsion system development schedule

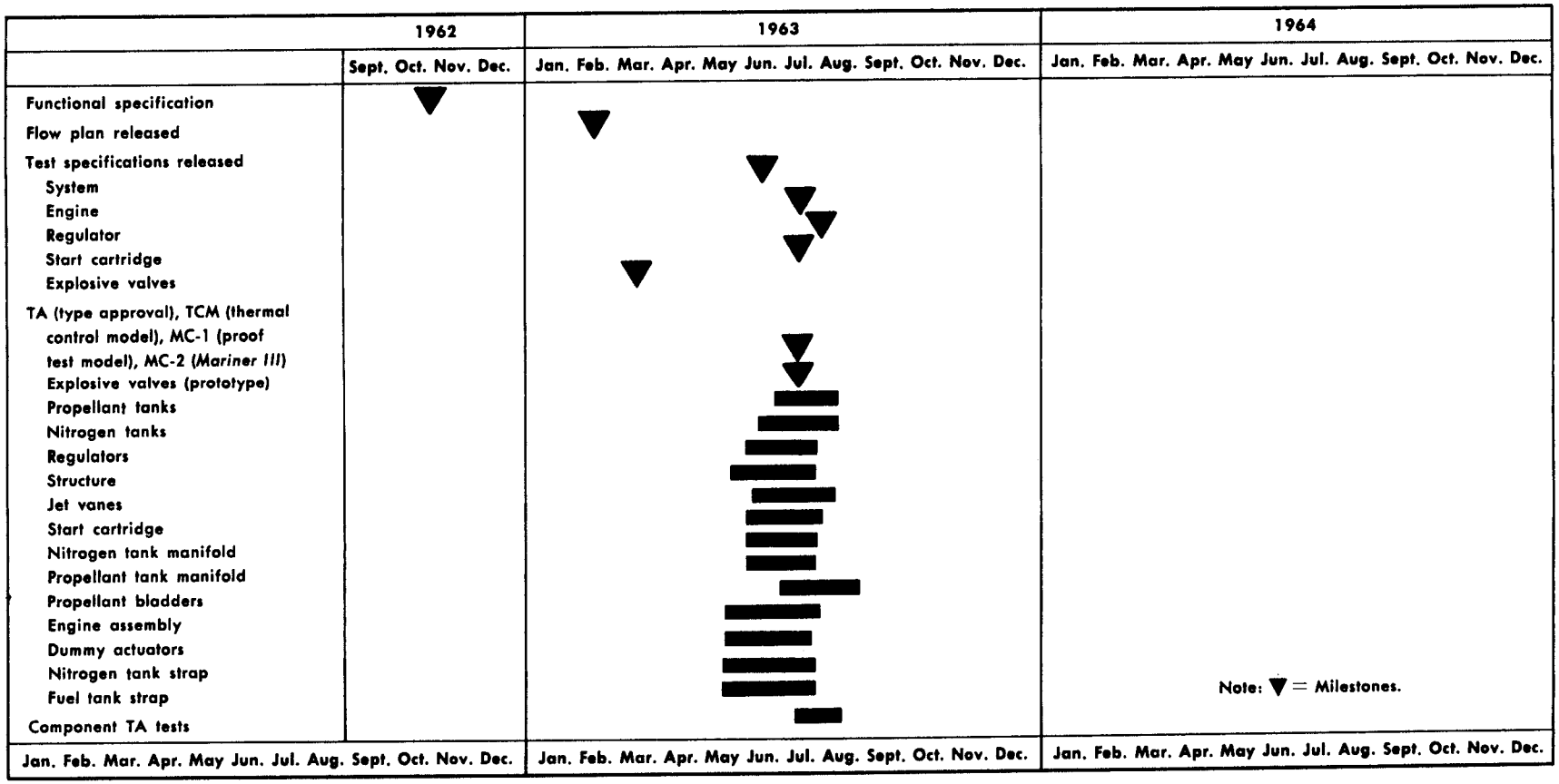

Table 4. Propulsion system development schedule (Cont'd)

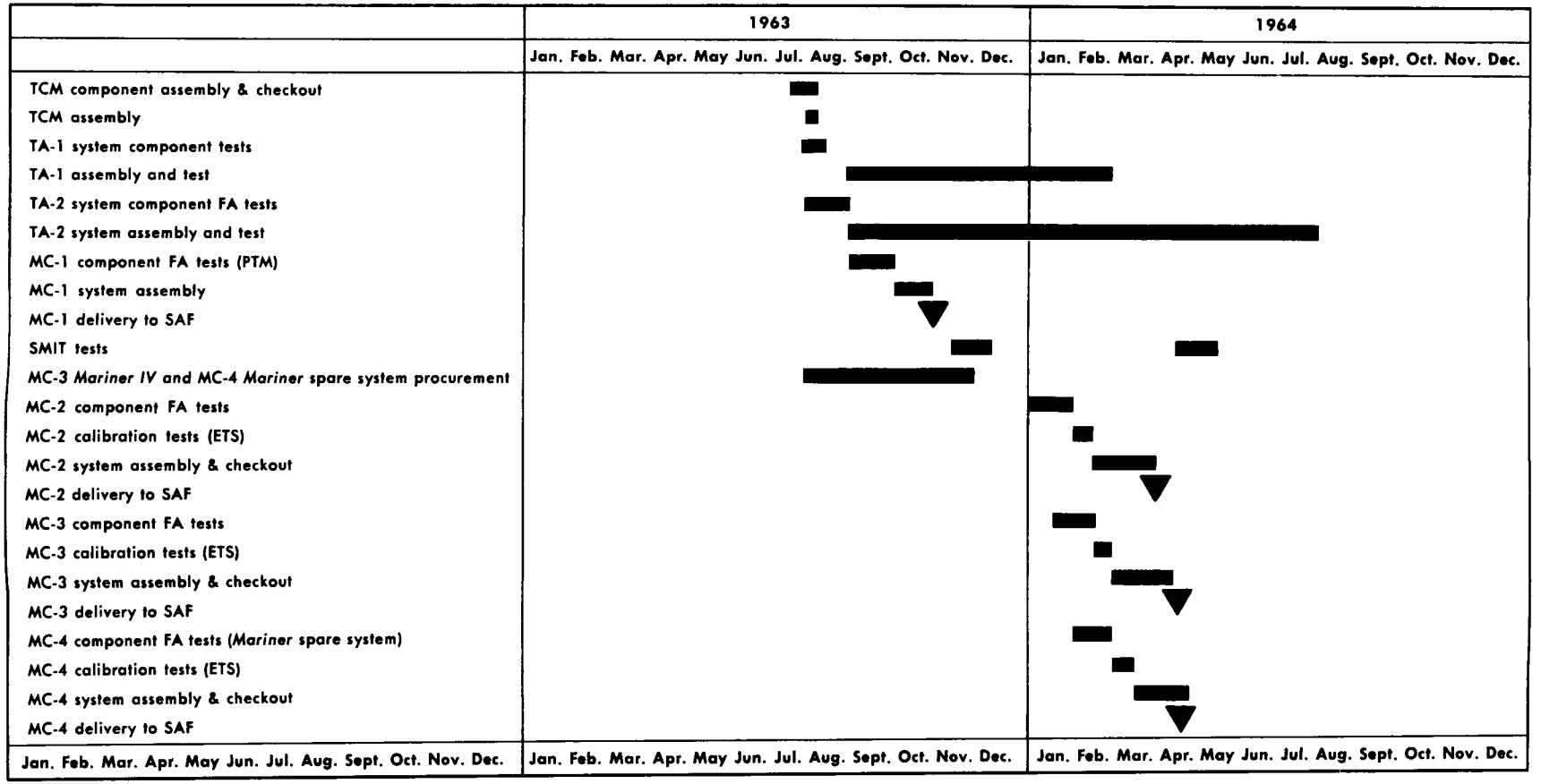

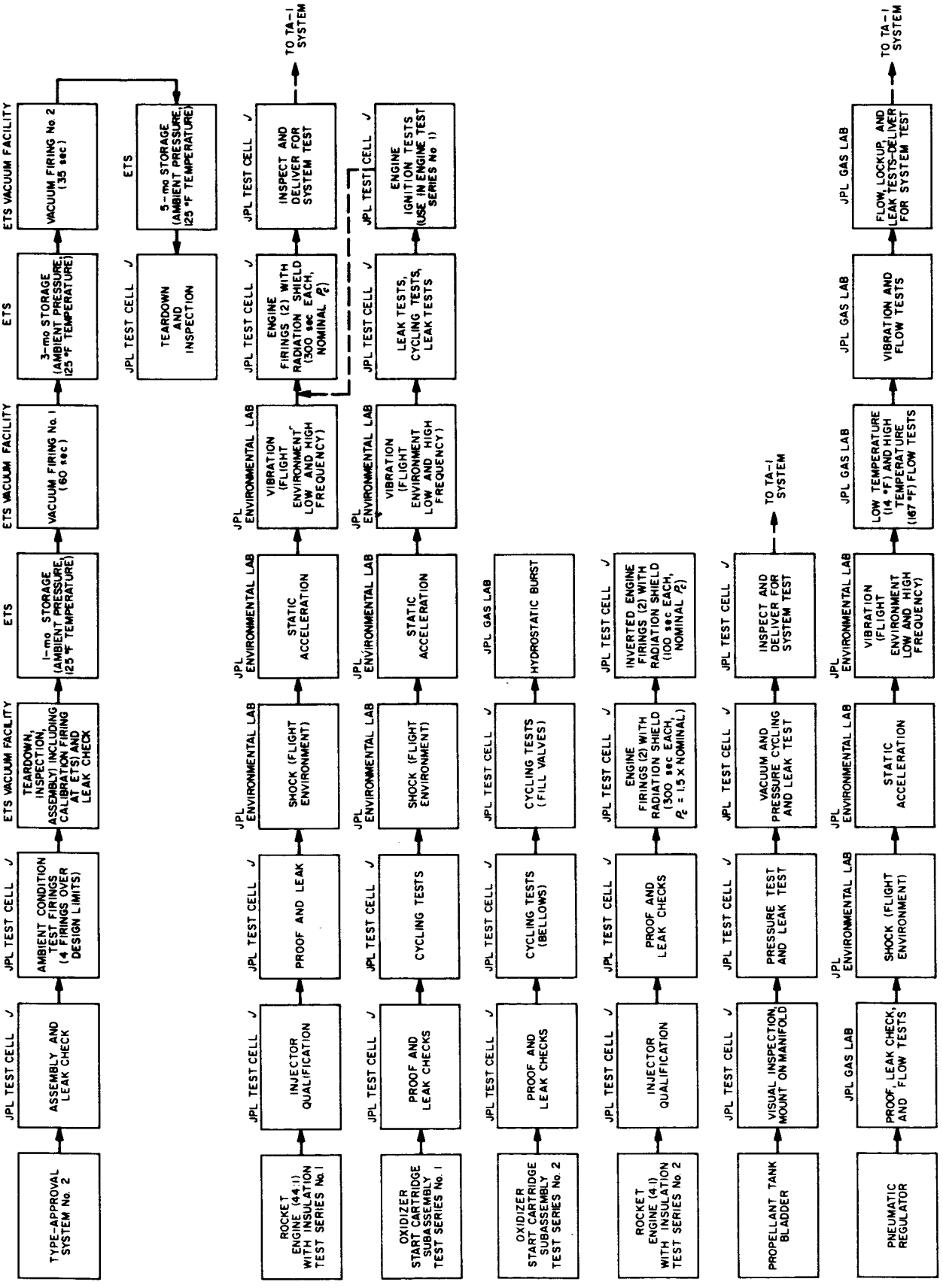

Fig. 7. Type approval test sequence

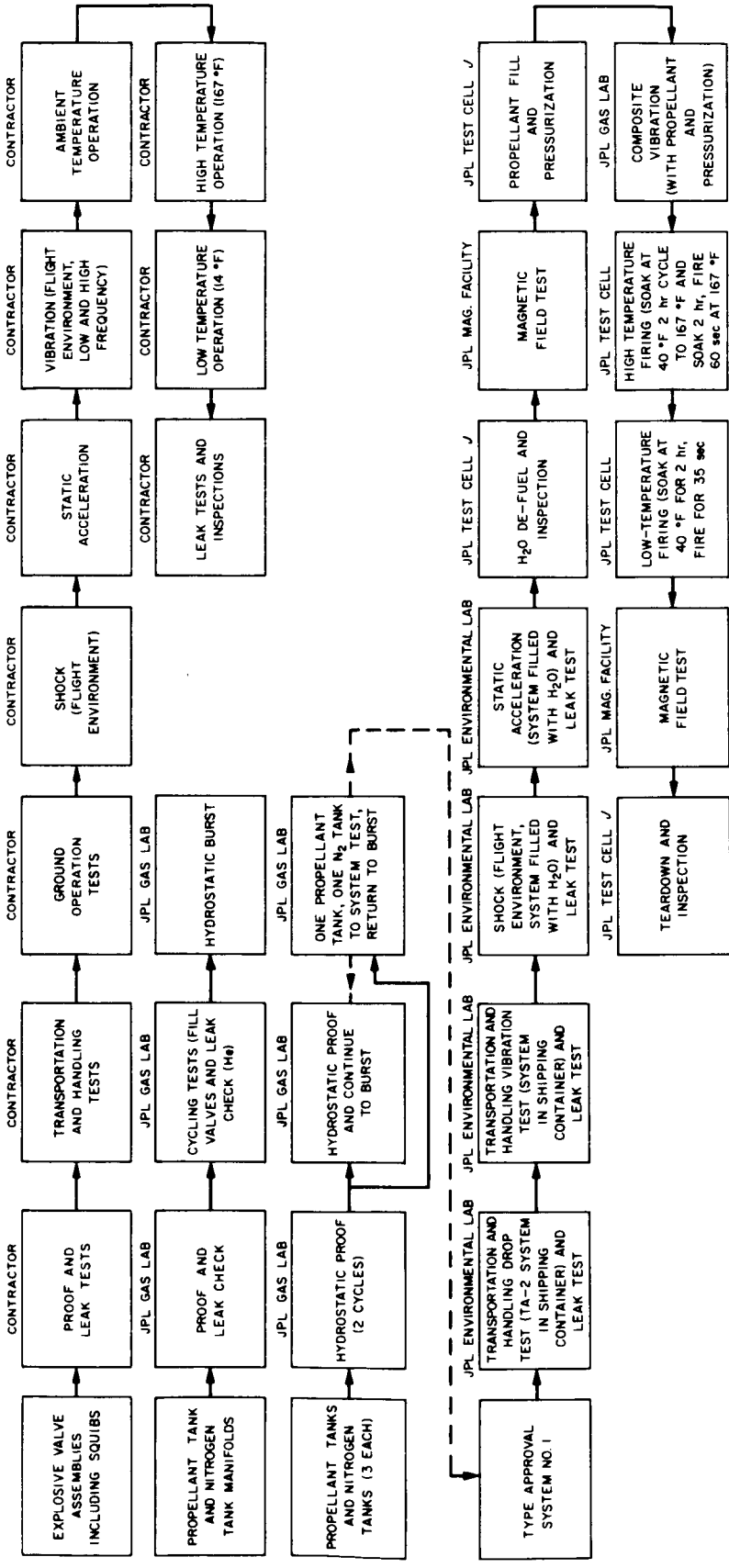
EXPLOSIVE VALVE ASSEMBLIES INCLUDING SQUIBS
PROPELLANT TANK AND NITROGEN TANK MANIFOLDS
PROPELLANT TANKS AND NITROGEN TANKS (3 EACH)
TYPE APPROVAL SYSTEM NO. 1
CONTRACTOR
PROOF AND LEAK TESTS
JPL GAS LAB
PROOF AND LEAK CHECK
JPL GAS LAB
HYDROSTATIC PROOF (2 CYCLES)
JPL ENVIRONMENTAL LAB
TRANSPORTATION AND HANDLING DROP TEST (TA-2 SYSTEM IN SHIPPING CONTAINER) AND LEAK TEST
CONTRACTOR
TRANSPORTATION AND HANDLING TESTS
JPL GAS LAB
CYCLING TESTS (FILL VALVES AND LEAK CHECK (He)
JPL GAS LAB
HYDROSTATIC PROOF AND CONTINUE TO BURST
JPL ENVIRONMENTAL LAB
TRANSPORTATION AND HANDLING VIBRATION TEST (SYSTEM IN SHIPPING CONTAINER) AND LEAK TEST
CONTRACTOR
GROUND OPERATION TESTS
JPL GAS LAB
HYDROSTATIC BURST
JPL GAS LAB
ONE PROPELLANT TANK, ONE N_2 TANK TO SYSTEM TEST, RETURN TO BURST
JPL ENVIRONMENTAL LAB
SHOCK (FLIGHT ENVIRONMENT, SYSTEM FILLED WITH H_2O) AND LEAK TEST
JPL TEST CELL J
TEARDOWN AND INSPECTION
CONTRACTOR
SHOCK (FLIGHT ENVIRONMENT)
JPL ENVIRONMENTAL LAB
STATIC ACCELERATION (SYSTEM FILLED WITH H_2O) AND LEAK TEST
JPL MAG. FACILITY
MAGNETIC FIELD TEST
CONTRACTOR
STATIC ACCELERATION
CONTRACTOR
LEAK TESTS AND INSPECTIONS
JPL TEST CELL J
H_2O DE-FUEL AND INSPECTION
JPL TEST CELL
LOW-TEMPERATURE FIRING (SOAK AT 40 °F FOR 2 hr, FIRE FOR 35 sec
CONTRACTOR
VIBRATION (FLIGHT ENVIRONMENT, LOW AND HIGH FREQUENCY)
CONTRACTOR
LOW TEMPERATURE OPERATION (14 °F)
JPL MAG. FACILITY
MAGNETIC FIELD TEST
JPL TEST CELL
HIGH TEMPERATURE FIRING (SOAK AT 40 °F 2 hr CYCLE TO 167 °F AND SOAK 2 hr, FIRE 60 sec AT 167 °F
CONTRACTOR
AMBIENT TEMPERATURE OPERATION
CONTRACTOR
HIGH TEMPERATURE OPERATION (167 °F)
JPL TEST CELL J
PROPELLANT FILL AND PRESSURIZATION
JPL GAS LAB
COMPOSITE VIBRATION (WITH PROPELLANT AND PRESSURIZATION)
RETURN PROPELLANT AND NITROGEN TANKS FOR BURST

Fig. 7 (Cont'd)

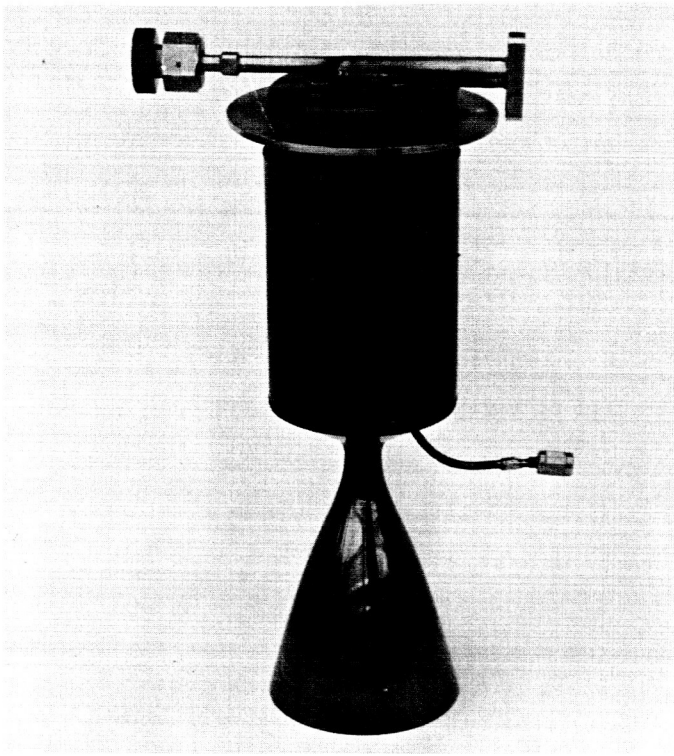

Fig. 8. View of *Mariner* C rocket engine

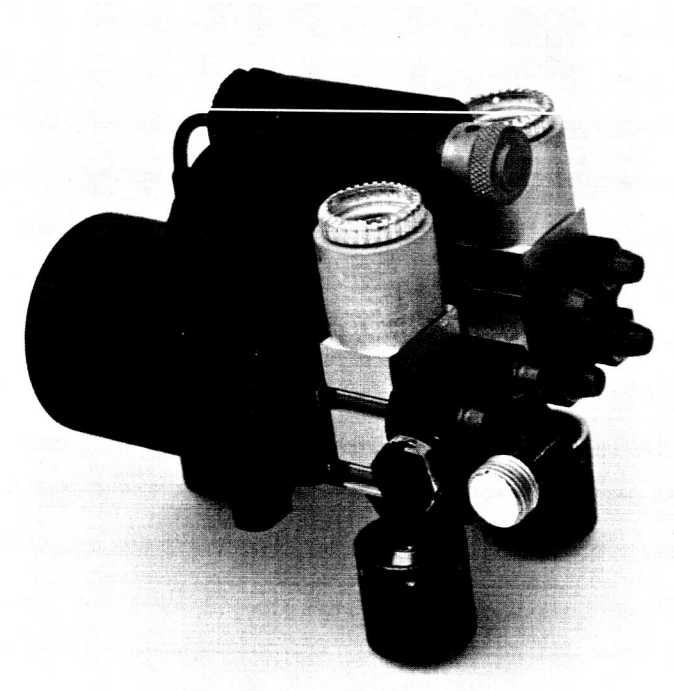

Fig. 9. Oxidizer start cartridge

two metallic bellows welded into a single housing. Normally closed explosive valves are connected to the outlet of the bellows with a check valve between them to prevent backflow of oxidizer from the second cartridge into the first cartridge during the second engine firing (see the system schematic in Fig. 1). The internal volume of each bellows contains approximately 15 cc of oxidizer. The exterior of the bellows is pressurized with gaseous nitrogen. When the explosively-actuated valve is fired, the nitrogen gas compresses the bellows, injecting the oxidizer into the engine for ignition.

3. Fuel Tank Bladder

A cell-type elastomeric bladder (Fig. 10) is used to accomplish fuel-positioning in a zero-*g* environment. The bladder material[5] was subjected to permeability and compatibility testing prior to fabrication. Permeability tests with the FR-6-60-26 compound indicated no measurable rates during a 90-hr test period. A compatibility test with the compound was made by immersing a sample of the material in a glass vial of hydrazine

[5]Compound FR-6-60-26, Fargo Rubber Co., Los Angeles, Calif.

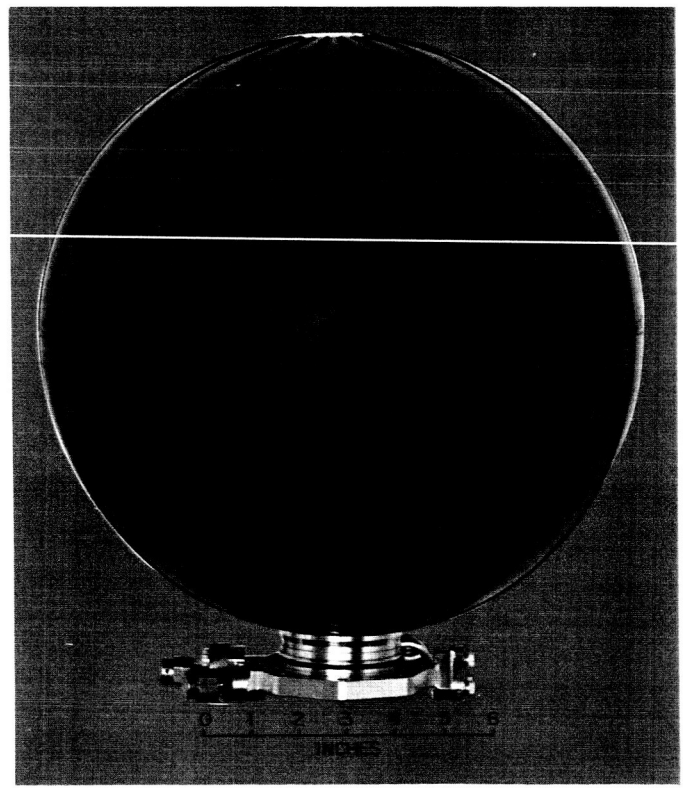

Fig. 10. External view of fuel tank manifold and bladder

at ambient temperature and measuring pressure rise as a function of time. At the end of 6-mo testing, the pressure rise was only 10 psi. Additionally, a fuel tank and bladder assembly was filled with hydrazine, pressurized, and stored at ambient conditions with the pressure being monitored on a daily basis. No pressure rise was noted during a 6-mo test period. The results of these compatibility tests indicated that the Fargo compound was adequate for the Mars mision.

Type approval testing of the bladder consisted of initial leak tests followed by 50 cycles of pressure-vacuum cycling. The bladder was then used in the TA-1 propulsion system TA tests described in Section IV-B.

4. Pneumatic Regulator

The pneumatic regulator for the *Mariner C* propulsion system is one of JPL design. The regulator is similar to that used on the *Ranger Block III* systems. The primary difference is that electron beam welding of the diaphragm is employed during manufacture to assure better seal characteristics. A cutaway view of the regulator is shown in Fig. 11. The regulator maintains a constant pressure to the fuel tank of the propulsion system, flowing nominally 0.006 lb/sec of gaseous nitrogen. During flow, the supply pressure may decay from 3600 to 360 psia while maintaining a constant outlet pressure (usually 310 psia). The regulator is capable of shutting off flow and maintaining a minimal leakage of 4 std cc/hr during this locked-up condition. The regulator is an all-metal, unidirectional-flow, normally open type and operates in the following manner: The variable inlet-pressure flows around the ball and seat into the low-pressure outlet chamber; impression of this pressure on the diaphragm's effective area results in controlled outlet pressure. Displacement during operation is accomplished by flexure of the diaphragm along with the mechanical backup configuration, and predetermined outlet pressure maintained by an equalizing force from the Belleville springs. The structural materials are primarily non-ferrous to minimize magnetic characteristics.

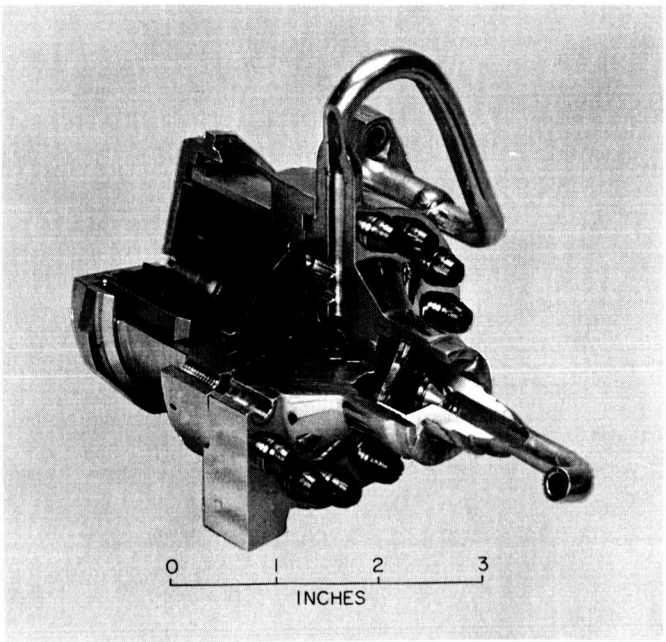

Fig. 11. Cutaway of pneumatic regulator

The TA test program consisted of initially undergoing proof, leak, flow, and lockup tests to assure proper operation of the regulator, prior to proceeding into the environmental testing (Fig. 7). The environmental tests consisted of shock, static acceleration, vibration, and temperature tests at 14 and 167°F. During, and after, each environmental test, the regulator was functionally operated to assure its correct operation.

During the early portions of the development program, considerable difficulty was experienced in meeting the internal leakage rate requirements, 4 std cc/hr, with the regulator in the closed condition. This problem was traced to contamination of the ball seat area by some particulate material emanating from a mesh filter located at the inlet of the regulator. The filter was redesigned to a labyrinth type, and no further difficulty was noted.

5. Explosive Valves and Squibs

Explosively actuated valves are used to accomplish all valving functions on the propulsion system. Because of the criticality of the explosive valve development, two designs were executed concurrently to assure that the flight hardware schedule commitments could be met. One design utilized two of the existing *Ranger* single-start explosive valves[6] in a parallel arrangement with an intermediate manifold. This design, which satisfies the *Mariner C* two-start requirement, represented a backup to the primary design. However, the *Ranger* valve internal seal design met only marginally the long-term space-storage requirements imposed by the *Mariner C* mission. Additionally, the squib used in the *Ranger* explosive valve experienced a seal problem (Ref. 2). Because of these shortcomings, the greatest effort was focused on development of a new valve–squib combination discussed below.

[6]Conax Corporation, Buffalo, New York.

The primary explosive valve design involved an entirely new approach utilizing an all-brazed construction which integrally manifolds two valves together in parallel.[7] Figure 12 shows a single oxidizer valve and Figs. 13 and 14 show nitrogen valves and fuel valves, respectively. In each case, the basic valve mechanism is identical.

[7]Pyronetics, Inc., Santa Fe Springs, Calif.

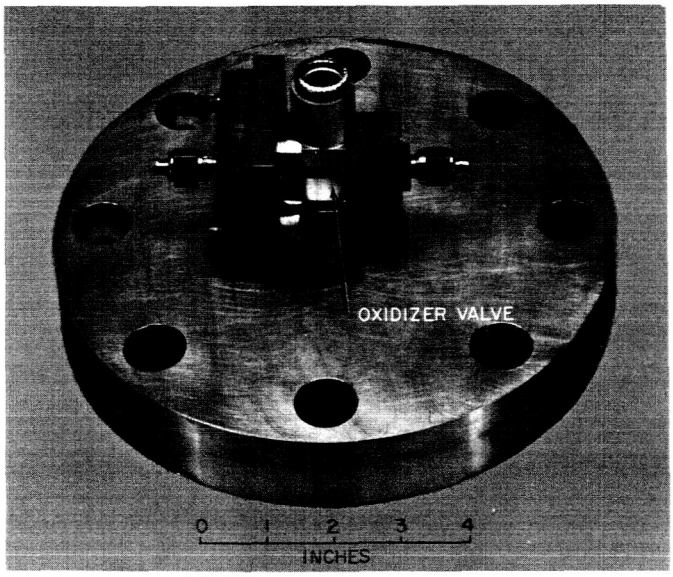

Fig. 12. Oxidizer valve mounted in test fixture

Early in the program, to assure the design adequacy of the valve-squib[7] combination, the vendor was directed to perform a feasibility test in which he was to double the nominal squib charge and demonstrate that the valve and squib would not suffer any damage. He was then to halve the nominal squib charge and demonstrate that the valve would still operate satisfactorily. During both series of tests, the valve operated satisfactorily, and all parts remained intact; however, venting of gases past the glass seal on the squib pins was noted on all tests. Gas venting of the squib was considered unsatisfactory because of possible contamination of optical surfaces on the spacecraft. Inspection of the fired squibs showed all the glass seals to be completely fractured. According to the glass manufacturers contacted, this extreme application requires the glass to be loaded in compression (the best load-bearing property of glass) rather than in pure shear, as designed. Therefore, this glass seal design could never maintain the squib pin-joint seal integrity. Additionally, two squibs failed to operate during the simulated midcourse interaction test (Ref. 3). On disassembly, the explosive charge materials were found intact. The few recovered bridgewire fragments appeared burned, but some fragments still welded at the pin were not even discolored. Inspection of the header revealed large voids in the braze material and the bridgewire end between the ceramic and the pin. Thus, it was concluded that the bridgewires were installed spanning the voids and were nicked by the exposed sharp ceramic edges along the voids when the propellants were pressed

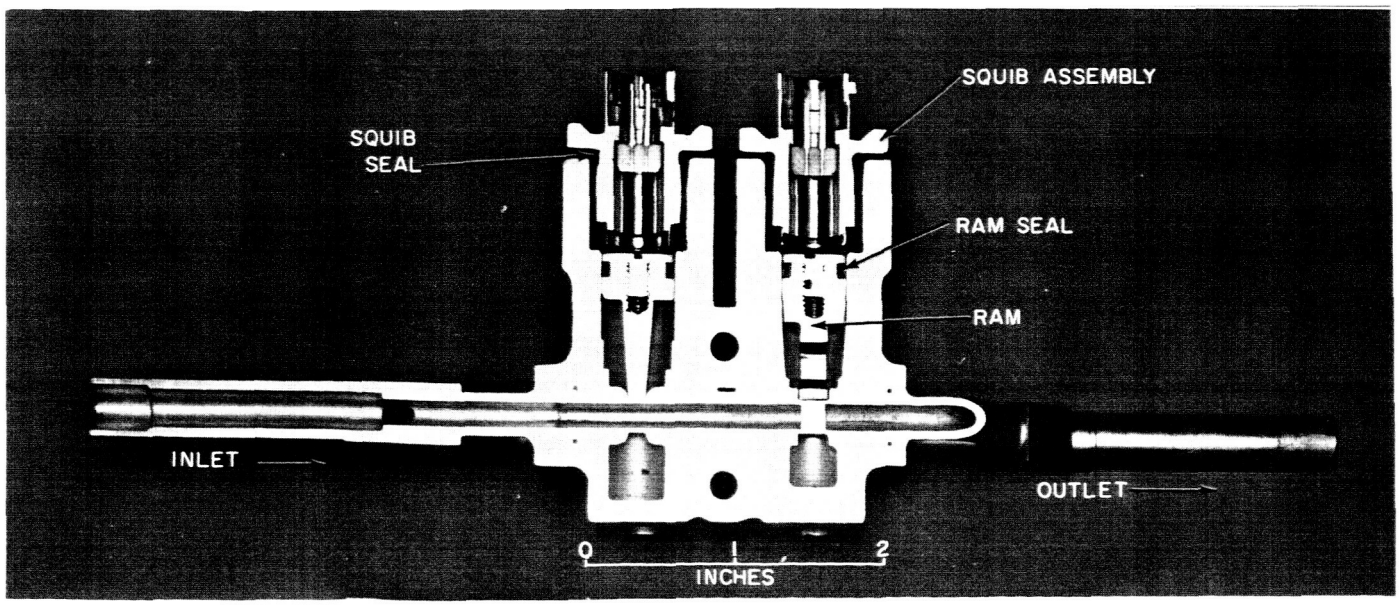

Fig. 13. Cutaway of nitrogen valve

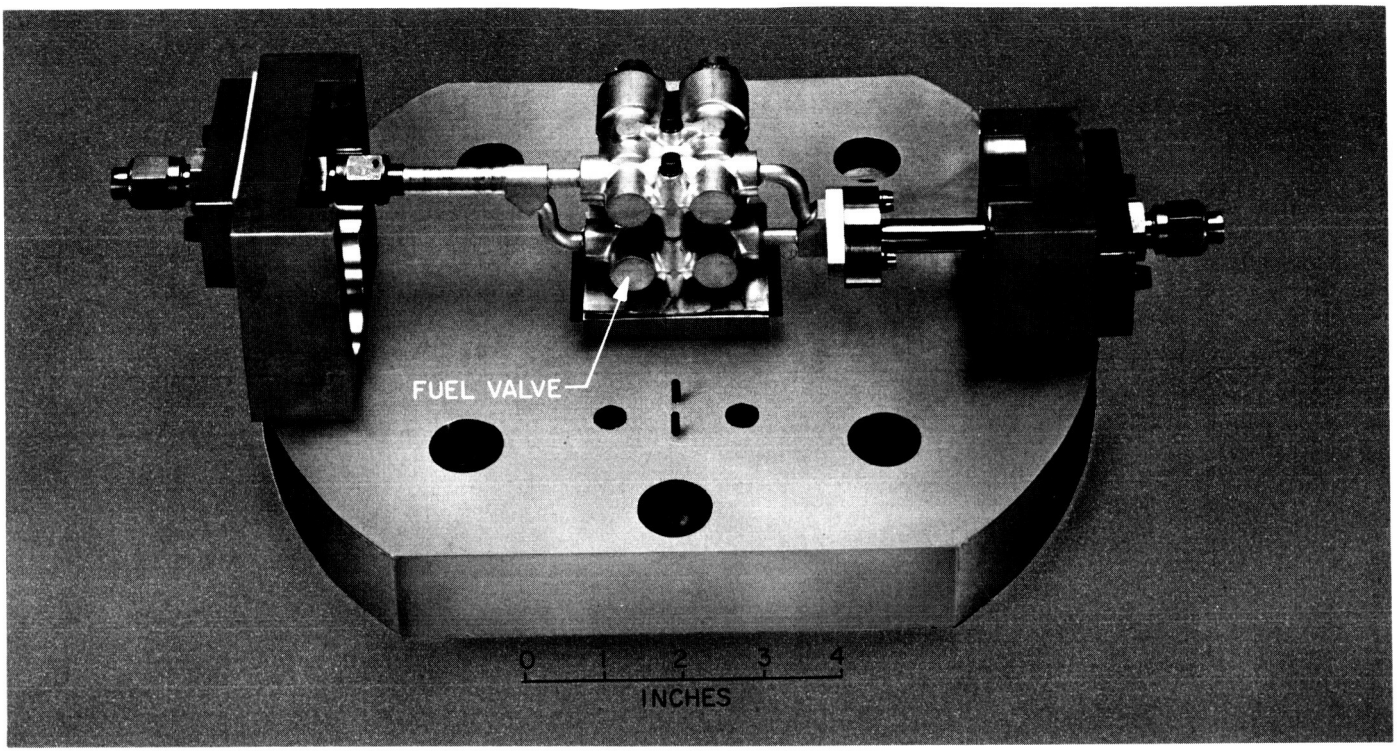

Fig. 14. Fuel valve mounted in test fixture

against the bridgewires with 13,000 lbf. It was postulated that the nicks, in turn, would increase local electric resistance and form hot spots at initiation, causing wire failure to shut off the electrical signal before sufficient energy could be transferred to the initiation charge materials. All of the above facts contributed to the decision to change squibs. The original squib[8] operated on a detonating principle. Analysis of the valve indicated that satisfactory operation should be obtained by a gas generating squib that develops an initial pressure of approximately 30,000 to 40,000 psia. A gas generating squib[9] was procured and evaluated to meet the above requirements, using the vendor's standard components to save program time. The evaluation consisted of fabricating four squibs each of five different charges: nominal, ½, 1⅓, 1⅔, and double charges. Firings were conducted in the Pyronetics valve. Two squibs of each group were fired at 14°F and two were fired at 167°F. During the nominal charge and ½-charge tests, normal valve operation was obtained and no venting of the squib gases was evident. During firing of the 1⅓-charge squibs the valve operation was normal, but two of the squibs exhibited slight leakage past the pin seal joint. During firing of the 1⅔-charge test the valve operation was normal, but one squib exhibited a slight gas leakage past the pin seal. During the double-charge, test gas leakage past the pins occurred on all four squibs, and in one case a pin blew out. During this test it was felt that the heat generated from the squib firing was great enough to melt the braze joint and was merely a quality control (QC) function. It was decided that these evaluation tests demonstrated that the gas-generating squib was superior to the one operating on the detonating principle. It was also decided that the slight pin leakage at the 1⅓ and 1⅔ nominal charge could be eliminated by improvements in the quality control procedures used in brazing the pins into the squib header. On the basis of these tests, the second squib tested was selected for valve actuation. These tests resulted in tightening QC procedures, and such additional non-destructive tests as X-raying of pin joints and nitrogen-gas proof testing during production were instituted.

As part of the development program on the explosive valve, it was originally planned to run a formal Bruceton test (Ref. 4) to determine the minimum squib charge required for valve actuation and the maximum charge allowable before valve or squib failure. Based on this data, the nominal squib charge would be chosen. However, the schedule did not allow for these tests to be performed so a best estimate of the charge was made

[8]Pyronetics manufactured.

[9]Hi-Shear Corp., Torrance, Calif.

based on the aforementioned evaluation of the Hi-Shear squibs. In place of the Bruceton test, a developmental test program was conducted wherein valves with maximum and minimum clearances were purchased, along with squibs whose charge was ½ nominal and 1⅔ nominal. The test program was designed so that the effects of under- and over-charge squibs could be evaluated with minimum and maximum clearance valves. All of these valve-squib combinations were subjected to TA testing. These tests were followed by functional tests of the valves at elevated temperatures (167°F). Approximately 110 valves were involved in this testing. In all cases, normal valve operation was obtained, which indicated that very adequate design margins existed with this valve/squib combination.

The formal TA program for the valves and squibs is indicated in Table 5. Two types of failure occurred during the TA program. First, a post-operation leak check of one oxidizer valve revealed a failure of the braze joint between the nipple and valve body. A failure of this joint allows leakage of chamber-pressure gases during engine operation. The location of the braze joint failure is shown in Fig. 15. An analysis of the joint indicated that it was underdesigned. The program schedule did not allow for its complete redesign; the solution to this problem was to add another serration concentric with, and outside of, the braze joint. This fix prevents external leakage if the braze joint fails. It was assured that the braze joint failure in no way compromised the functional reliability of the valve. The new seal design was successfully demonstrated as preventing external leakage and the valve was considered to be qualified for flight.

The other type of failure occurred during the squib portion of the type approval tests. Two squibs fired when they were subjected to the static discharge test of 10 kv from a 300 pf capacitor. Approximately 100 squibs were subjected to this test. Analysis of the failure revealed that the circuitry used in conducting the test had a resonance condition such that the squib was actually being subjected to twice the desired test voltage. Analysis of the squib insulation indicated that voltages of approximately 20,000 to 25,000 v could puncture the insulation and, thus, lead to a squib failure. The circuitry used for this test was modified to eliminate the resonance condition, and no further problems were encountered.

6. Tankage

The propellant and nitrogen tanks on the propulsion system are made of 6A1-4V titanium alloy (Fig. 16). The propulsion system design dictated minimum burst pressures of 945 psia for the propellant and 7265 psia for the nitrogen tank.

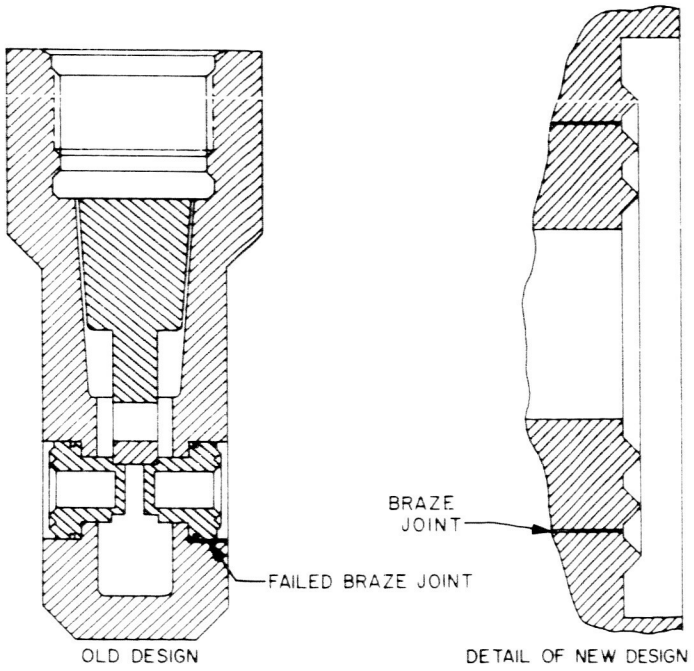

Fig. 15. Cross-section view of oxidizer explosive valve

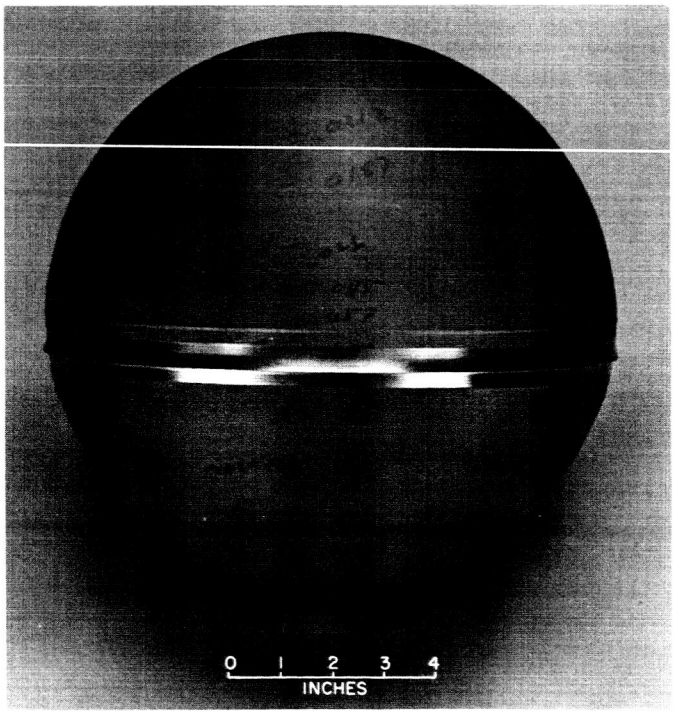

Fig. 16. Fuel tank shell

Table 5. Explosive valve and squib type approval tests

a. Preflight and boost phase

Test sequence	Number of units	
	Squibs	Valves
Examination		
Magnetic inspection	175	11
Radio graphic examination	175	11
Weight	175	11
Electrical performance		
Bridge wire resistance test A	175	11
Dielectric strength of squibs	175	11
Dielectric resistance of squibs	175	11
Resistance of squib shields	175	11
Mechanical performance		
Leak test of squibs	12	11
Proof pressure-valve bodies	—	11
Leak test A	—	11
Bridge wire resistance	—	11
Pyrotechnic performance, squib		
No-fire pulse	—	—
Static discharge	117	—
No fire	78	—
50% firing curve	6	—
50% no-fire	6	—
50% all-fire	6	—
Auto ignition temperature	6	—
High temperature deterioration	10	—
Temperature shock I	90	—
Bridge wire resistance, test A	10	—
Dielectric strength	10	—
Dielectric resistance	10	—
Transportation and handling		
Drop test A	10	—
Drop test	54	11
Bench handling	—	11
Transportation vibration	54	11
Bridgewire resistance, test A	—	11
Ground operation		
Humidity	32	11
Salt fog	20	11
RF interference	—	11
Leak test of squibs	50	—
Leak test A	—	11
Bridgewire resistance, test A	50	11
Flight environment, boost phase		
Shock	55	11
Static acceleration	55	11
Vibration test I	30	11
Magnetic inspection	—	11
Temperature-altitude	16	—
Leak test B	—	11
Bridgewire resistance, test A	95	11

b. Space flight phase and post-flight

Test sequence	Number of units	
	Squibs	Assemblies
Flight environment, space flight phase		
Space flight temperature	—	11
Leak test B	—	11
Electrical performance	20	11
Assembly operation (ambient)	—	5
Leakage test D	—	5
Bridgewire resistance, test A	—	5
Assembly operation (high temperature)	—	2
Leakage test D	—	2
Bridgewire resistance, test A	—	2
Assembly operation (low temperature)	—	4
Leakage test D	—	4
Bridgewire resistance, test A	—	4
Pressure drop	—	7
Shock (post operation)	—	12
Leak test C	—	12
Bridgewire resistance, test A	—	12
Dielectric strength	—	12
Dielectric resistance	—	12
Flight coast		
Pre coast test I	—	4
Low pressure coast—ambient test II	—	2
Low pressure coast—thermal cycling test III	—	2
Leak test E	—	9
Proof test	—	2
Minimum burst	—	2
Ultimate burst	—	2
Pyrotechnic performance, supplemental		
Magnetic inspection	85	—
Squib no fire pulse	80	—
Electrical performance	95	—
Squib no fire	—	—
Leak test squib	—	—
Temperature—shock I	—	—
Bruceton no-fire	25	—
Sampling all-fire	40	—
Squib operation		
Ambient	—	—
High temperature	6	—
Low temperature	5	—
Integrity (squib & guard)		
High temperature	5	—
Low temperature	5	—
Disassembly and inspection	—	12
Storage	20	12

Three propellant tanks and three nitrogen tanks were subjected to type-approval testing. Each tank was hydrostatically proof-pressurized to 1.5 times its maximum operating pressure through three cycles, and pressure volume measurements were made. On the third cycle, two each of the nitrogen and propellant tanks were subjected to continued pressure to burst at a rate computed to best show the pressure effect on the tank. The third propellant and nitrogen tanks underwent type-approval testing with the complete TA-1 propulsion system. On completion of the system type-approval tests, the tanks were again subjected to three cycles of proof test with the pressure being carried to the burst pressure on the third cycle. Test results indicated that the minimum burst pressure was 972 psia for the fuel tank and 7370 psia for the nitrogen.

7. Fill Valves

In contrast to the *Ranger* fill valve concept (Ref. 2) a new JPL technique was employed on this system (Ref. 5). Figure 17 is a sectioned view of the fill valve assembly. This valve consists of a stainless steel screw which presses a ceramic ball against a central hole in an internally threaded aluminum or stainless steel boss. The ceramic ball (burnished with molybdenum disulfide powder, which serves as a dry lubricant) is retained on the end of the screw with a circumferential-swage fit.

The valve is opened by backing the ball off the seat. This is done by turning the screw with a special tool. The valve is closed by screwing the valve shut so that the ball is seated; a net torque of 10 in.-lb is required. During the time that the ball is in contact with the seat, there is no scrubbing or relative motion between the ball and seat because the ball pivots on the flat bearing surface on the screw; this is an important feature, because it minimizes scratching, galling and wear.

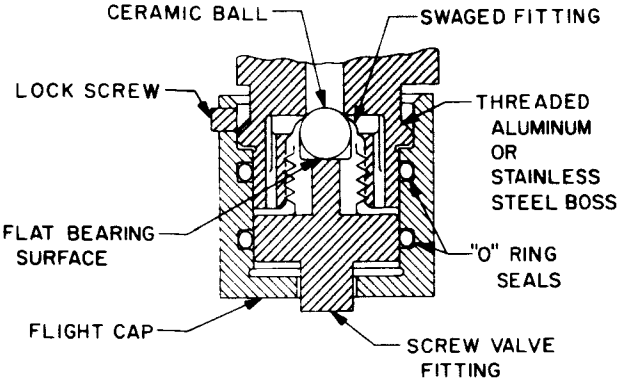

Fig. 17. Sectioned view of fill valve assembly

A non-flight ground-support fitting, which is pressure balanced, is held in place over the boss by two "O" rings. The flight-type pressure-balanced cap is held in place by two "O" rings, also, but these rings are redundant seals, only.

C. System Type-Approval Tests

Two propulsion systems were subjected to type-approval testing (Fig. 7). One system, designated TA-1, was assembled of components that had previously passed either TA or FA tests. This system was then subjected to environmental tests, as detailed in the ensuing paragraphs. A second system, the TA-2, was assembled of components that previously had passed FA testing, and complete system firings over the design limits of initial tank pressurization levels were conducted. On completion of the TA-2 system firings, the system was used in a life-storage test.

1. TA-1 System

After assembly of the TA-1 propulsion system, it was subjected to a series of modal tests; a typical test setup is shown in Fig. 18. This series of tests was to determine the structural resonant frequencies and the corresponding modes of vibration. Very low vibration levels were fed into the structure at various frequencies until the resonant points were found. Readings taken from accelerometers mounted at various points on the structure were used to define the mode shapes. There was very good correlation between the actual test data and the analysis on which the structural design was based. On completion of the modal tests, the TA-1 system was subjected to a series of preliminary vibration tests to determine amplification factors at selected points on the structure. Vibration levels from 0.5 *g* rms to 2.5 *g* rms were fed into the system sweeping at frequencies of 50 to 400 cps. The first resonant frequency of the structure was at approximately 140 cps, at which frequency, an amplification factor of 5 was measured at the center of gravity of the structure. The TA-1 system was subsequently installed in a shipping container similar to that shown in Fig. 19 and subjected to the transportation and handling, drop and vibration tests. The system was then removed from the shipping container and subjected to the space-flight shock test and the static acceleration test. After each of the tests, a thorough leak check was performed on the system; no leakage or other system failures were noted.

Next, the start cartridge was filled with nitrogen tetroxide, the propellant tank was filled with water to

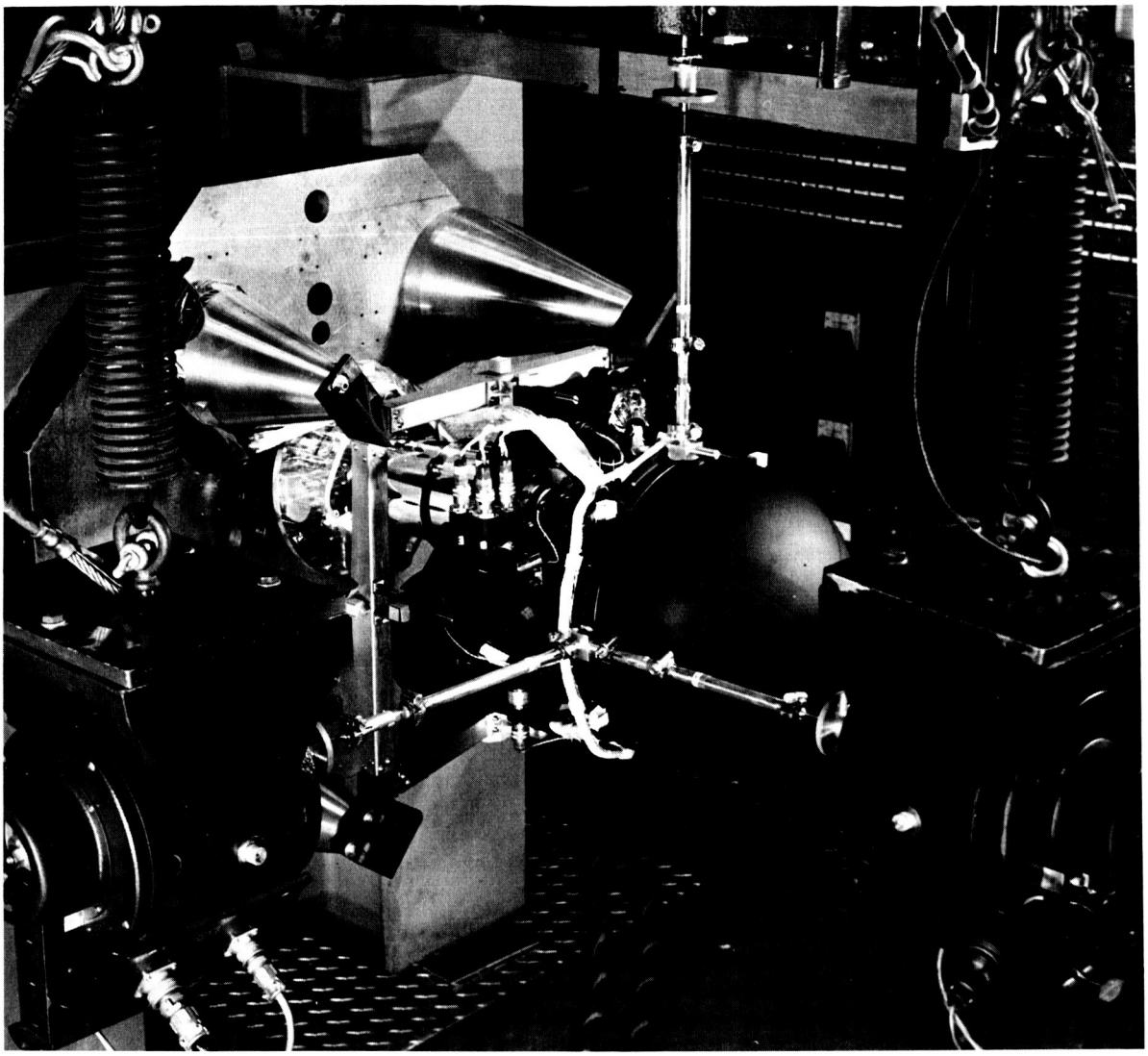

Fig. 18. Test configuration for modal vibration of TA-1 propulsion system

simulate the propellant, the system tankage was pressurized to the maximum expected flight values in preparation for the boost-phase vibration test. Immediately before the test, a 1-g input was fed into the propulsion system and a frequency sweep was made from 20 to 2000 cps. During this frequency sweep, very high acceleration levels were noted at the fuel tank attachment point when the structure resonant point was reached. The amplification factor was a factor of 10 higher than had been noted on the preliminary vibration tests in which the tankage was not pressurized. Apparently, the introduction of a gas at high pressure between the propellant-tank wall and the propellant-expulsion bladder (the bladder contains 21.5 lb of hydrazine) inhibits sloshing of the propellant. Since sloshing contributed to damping by dissipating energy, inhibiting sloshing resulted in markedly higher amplification factors throughout the propulsion system. At this point it was felt that the propulsion system could not pass the formal type-approval vibration test if this high amplification factor existed when higher vibration levels were applied.

To ascertain the quantitative effects of various pressurization levels and acceleration input levels, a number of tests were made with a propulsion system similar to TA-1. Frequency sweeps were from 50 to 150 cps, tank pressures were 0, 150, 275, and 395 psig; and input accelerations varied from 1- to 5-g rms. As expected, the amplification factor went up with pressure and down with increasing input acceleration. The amplification

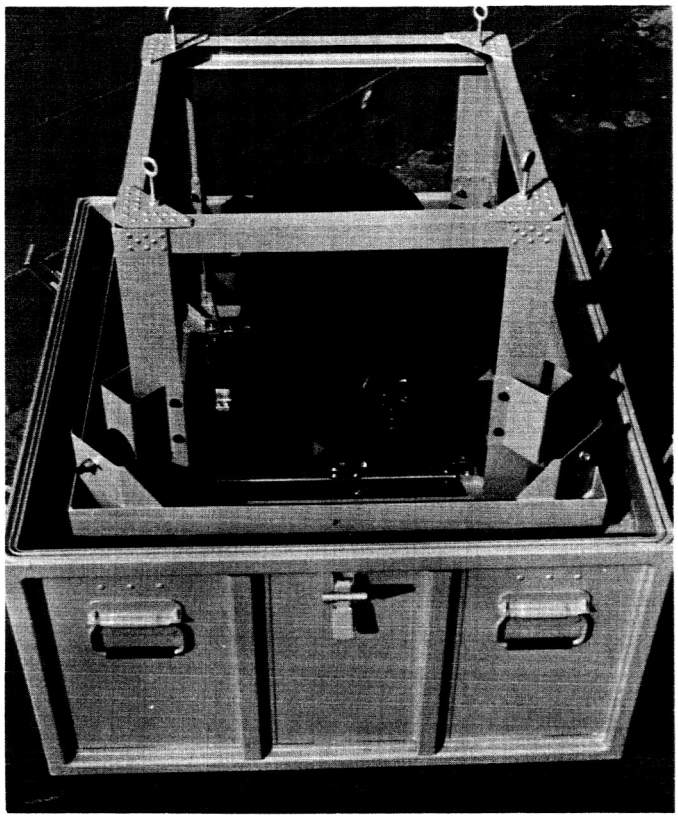

Fig. 19. Shipping container for propulsion system

factor at the propellant tank support ring and the propulsion system support structure are typical; they are tabulated in Table 6.

The results of the system vibration testing, plus results from the structural test model (STM) spacecraft testing that indicated that the input levels to the propulsion system were actually lower than originally expected, indicated that the system could pass the formal revised TA vibration tests. The actual test levels and sequence in which the TA-1 system was tested were as follows:

1. A 2.5 g rms sinusoid from 20 to 100 and back to 20 cps (10 min)

2. White Gaussian noise, power spectrum density (PSD) of 0.20 g^2/cps from 300 to 1000 cps, with a 6 db/octave rolloff from 1000 to 2000 cps, a 3 db/octave rolloff from 300 to 20 cps, and 24 db/octave rolloff below 30 and above 2000 cps (3 min)

3. White Gaussian noise, PSD of 0.010 g^2/cps, band-limited between 100 and 2000 cps, plus a 2.5-g rms sinusoid superimposed on the noise sweeping from 100 to 450 and back to 100 cps (10 min)

Table 6. Summary of vibration testing on a typical *Mariner* C propulsion system

Input acceleration, g rms	Propellant tank pressure, psig	Resonant frequency, cps	Tank ring amplification factor	Substructure amplification factor
Vibration perpendicular to rocket engine thrust axis				
1	0	78	2	6
1	150	78	6	15
1	275	74	8	23
1	395	72	9	26
2	150	74	5	12
2	395	68	6	18
3	150	72	4	10
3	395	64	5	14
4	150	66	4	9
4	395	64	5	18
5	395	64	5	16
Vibration parallel to rocket engine thrust axis				
1	0	118	2	6
1	150	108	10	22
1	275	104	12	30
1	395	102	18	45
2	150	104	8	19
2	395	102	13	32
3	0	104	2	5
3	150	96	8	18
3	395	96	10	23
4	150	92	8	18
4	395	92	8	16
5	395	94	8	9

4. White Gaussian noise, PSD of 0.010 g^2/cps, band-limited between 100 and 2000 cps, plus an 8-g rms sinusoid superimposed on the noise sweeping from 450 to 2000 and back to 450 cps (10 min)

For steps 1, 2, and 4, the sweep through the frequencies is controlled such that time rate of change of frequency increases directly with frequency. The tests were conducted in three axes—one parallel to the thrust axis and in orthogonal axes normal to the thrust vector.

No structural damage was noted during the vibration tests on the TA-1 system. After completion of the vibration tests, the system was subjected to temperature tests and then fired while at temperature. Figure 20 is a schematic representation of the test configuration. The first test consisted of a 2-hr soak at 40°F followed by an additional 2-hr soak at 167°F. The system was then fired for 60-sec duration while at 167°F. Nominal system performance was obtained during the test. The system was

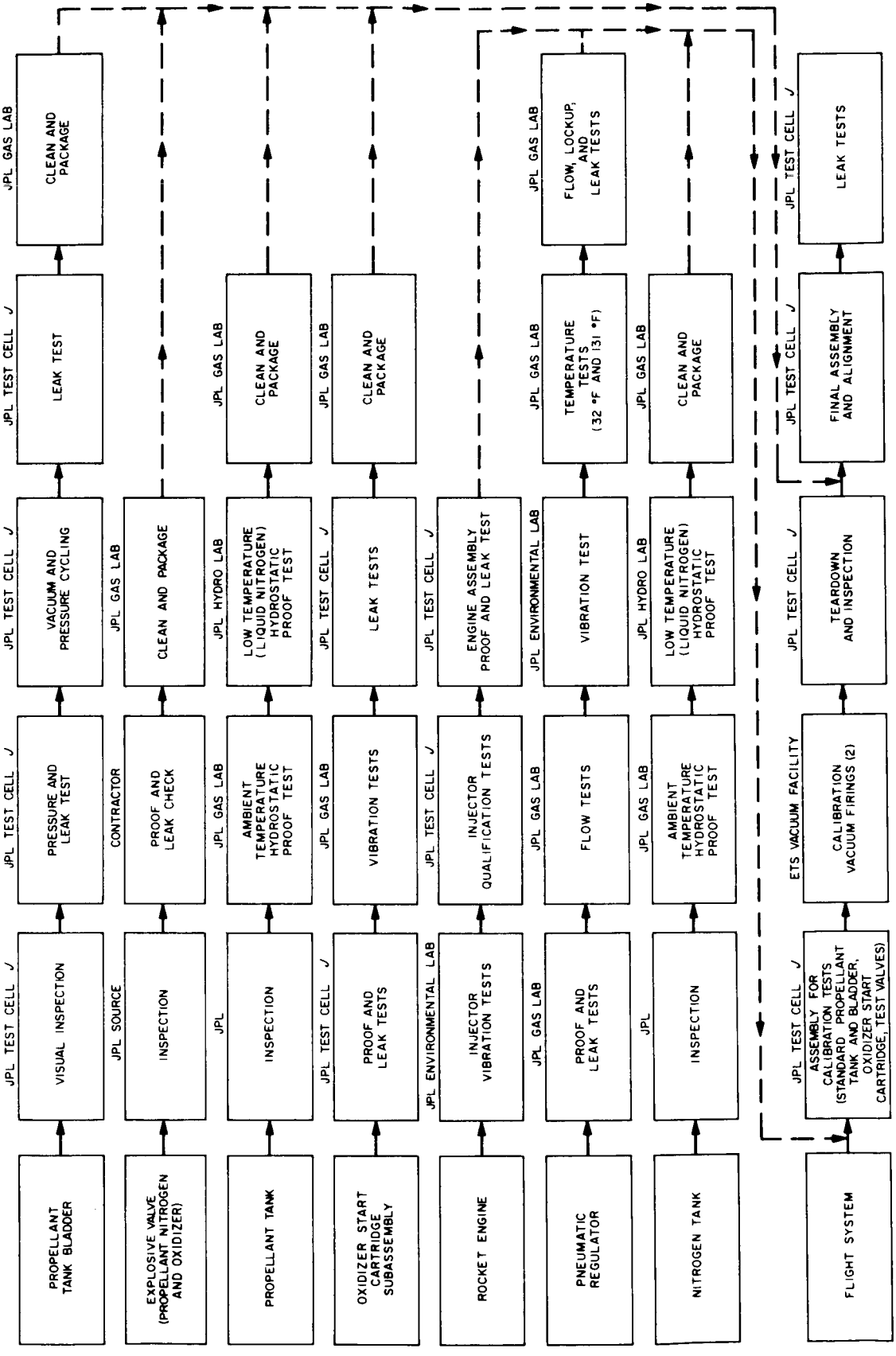

Fig. 20. Flight acceptance test sequence

then soaked at 40°F for 2 hr and then successfully fired for 30-sec duration.

2. TA-2 System

The TA-2 propulsion system was built up from components which had previously passed FA testing (Fig. 7). The testing on this propulsion system consisted of conducting firings at various tank pressures so as to define system start transients and steady-state operation under a variety of starting conditions. For the first test, all tanks were pressurized to their nominal values (propellant tank 304 psia, nitrogen tank 3000 psia, and start cartridge 400 psia). The first test was of 80-sec duration and the resulting performance was very close to that predicted for the system. For the second firing of the system, the initial pressures were those remaining from the previous test at shutdown (333 psia in the propellant tank, 368 psia in the start cartridge and 1300 psia in the nitrogen tank. Nominal performance was obtained from this 15-sec test. After the second test, the explosive valves were replaced, and the system was refilled with propellants. For the third test, the tanks were pressurized to their maximum-expected flight values (propellant tank 410 psia, nitrogen tank 3300 psia, and start cartridge 445 psia). The third test of 95 sec, again was normal. The system was then refueled, and a fourth test at low tank prepressurization levels (propellant tank 125 psia, nitrogen tank 2800 psia, and start cartridge 345 psia) was attempted. The system was shut off after 14 sec, when it was observed that the pressure regulator had malfunctioned and did not regulate until the propellant tank pressure had reached 500 psig. Post-run examination of the regulator indicated that a considerable quantity of 25-μ particles had been deposited on, and had caused damage to, the regulator seat area. These particles emanated from firing of nitrogen explosive valves located upstream of the pressure regulator. Normally, a filter is contained upstream of the regulator and it serves to prevent particle contamination of the pressure regulator. However, at the time this pressure regulator was being qualified, considerable difficulty was being experienced in obtaining clean filters (see Section III). To prevent delay of system firings, it was decided to fabricate the pressure regulator for the TA-2 system without a filter, since it was felt that the danger from particle contamination of the dirty filters (which could not be successfully cleaned) was as great as contamination from the explosive valves. Another regulator with a good filter was assembled into the TA-2 system, and the fourth test of the series was successfully completed. After this test a repeat of the third test of the series provided good results.

3. Life Test

Following the TA-2 system tests, the system was disassembled and reassembled with new components that had previously passed flight acceptance testing. Prior to the assembly, the rocket engine and pneumatic regulator were installed in a standard calibration system and subjected to a thrust calibration test in the same manner as that of the flight systems. Two tests—one 60 sec and one 30 sec—were conducted in a high altitude facility. System total impulse, as well as other system operating parameters, was measured during the test and supplied data that could be compared with system firings conducted during the life test.

When the system was assembled, it was filled with propellants and pressurized to the nominal flight levels, then installed in a storage trailer, where ambient temperature was maintained at 125°F. During the first month of storage, a pressure rise of approximately 1.5 psia/day was noted in the fuel tank, indicating incompatibility between the bladder and hydrazine. At the end of this 1-mo storage, the system was removed from the trailer, installed in a high altitude facility, and test fired for 60 sec. Normal system operation was obtained. The total impulse measured was within 3% of the value obtained during the calibration test previously described. This value was well within the required 3σ impulse reproducibility.

After firing, the unit was reinstalled in the storage trailer at a temperature of approximately 120°F. The same rate of pressure rise in the fuel tank was again noted. After a total of approximately 3½-mo storage time, the temperature was lowered to 90°F to determine the effect of the lower temperature on the rate of fuel-tank pressure rise. As was expected, no pressure rise was noted during the following two weeks, confirming that the pressure rise rate was very temperature-dependent. Other testing had indicated that the rate changed by a factor of 3 for each 10°F change in temperature (Ref. 6). The 90°F temperature was still 50% above the expected flight temperature.

After a 4-mo storage, the unit was test fired a second time for 30 sec. The total impulse measured was within 0.2% of that obtained during the previous 30-sec calibration test. The system was again installed in the storage trailer at 120°F. For the next 2 mo, the fuel tank pressure again continued to rise at 1.5 psia/day. Following a total of 6-mo storage time, the temperature

was reduced to 100°F and was held between 80 and 100°F for an additional 4 mo; there was no evidence of fuel tank pressure rise.

Throughout the 10-mo storage, the nitrogen tank pressure remained constant with no measurable leakage being noted. At 2½ mo after the start of the life test, a drop of approximately 4 psia/day was noted in the start cartridge. This pressure-loss indication suggested a failure either of the metal bellows within the start cartridge or of the pressure transducer. Placement of a visual pressure gauge on the start-cartridge/nitrogen reservoir revealed that the pressure in the cartridge was actually remaining constant. Subsequent investigation revealed that a bourdon tube braze joint in the pressure transducer had failed and was allowing pressure to leak into the sealed cavity of the transducer. Thus, as the pressure in the transducer cavity increased, the differential pressure across the bourdon tube decreased, so that a pressure loss was indicated. Although the braze joint had previously been recognized as a problem and had been redesigned, when the life test began, the redesigned unit was not available.

In summary, the life test proved that the system could be stored for prolonged periods of time, then fired, and that the system total impulse was repeatable within the required limits. The test indicated that compatibility of the fuel tank bladder and hydrazine can become a problem if the system temperature approaches 120°F while in flight. The design adequacy of the seals used in the system was well verified; no leakage, other than the pressure transducer failure, was noted.

V. FLIGHT-ACCEPTANCE TESTING

A. Component Level Flight-Acceptance Tests

Since a timer-shutoff mechanization was employed, the flight-acceptance (FA) testing at the system level deviated from that conducted with previous systems of this general design (*Ranger* and *Mariner Venus*). The following paragraphs describe the FA test history of the system components and system assembly (see Fig. 21).

1. Rocket Engine

The catalyst used in the rocket engine is prefired for 30-sec duration in a standard test chamber to assure its correct operation and to eliminate any structurally weak catalyst particles. The injector of the engine is subjected to water flow testing to ascertain that its flow characteristics are within specification. The injector is then subjected to FA vibration testing. Following the vibration testing, the injector is leak checked and then test-fired in a standard test chamber. During the test firing the injector performance and smoothness of operation must be within specified limits. Final weldment of the engine assembly occurs upon completion of engine proof and leak tests. After approval of the X-rays of the weld joints, the engine is considered ready for the system level testing.

2. Oxidizer Start Cartridge

Following weldment of the start cartridge it is subjected to extensive proof and leak tests to verify the soundness of the metal bellows. The assembly is then filled with water (to simulate the propellant) and subjected to FA vibration testing. Following the vibration testing the component is leak checked, final cleaned, and considered ready for installation on a flight system.

3. Fuel Tank Bladder

The fuel tank bladder is subjected to initial leak tests which consist of pressurization with 1 psig of gaseous nitrogen and immersion in a water bath to observe for leakage. The bladder is then subjected to five vacuum-fill cycles and the leak-test is repeated. Upon successful completion of this leak-test the bladder undergoes final cleaning and is considered ready for installation into the fuel tank.

4. Pneumatic Regulator

After the regulator is assembled and final adjustments are made, the unit undergoes a series of flow and lockup tests. These tests are followed by FA vibration tests and

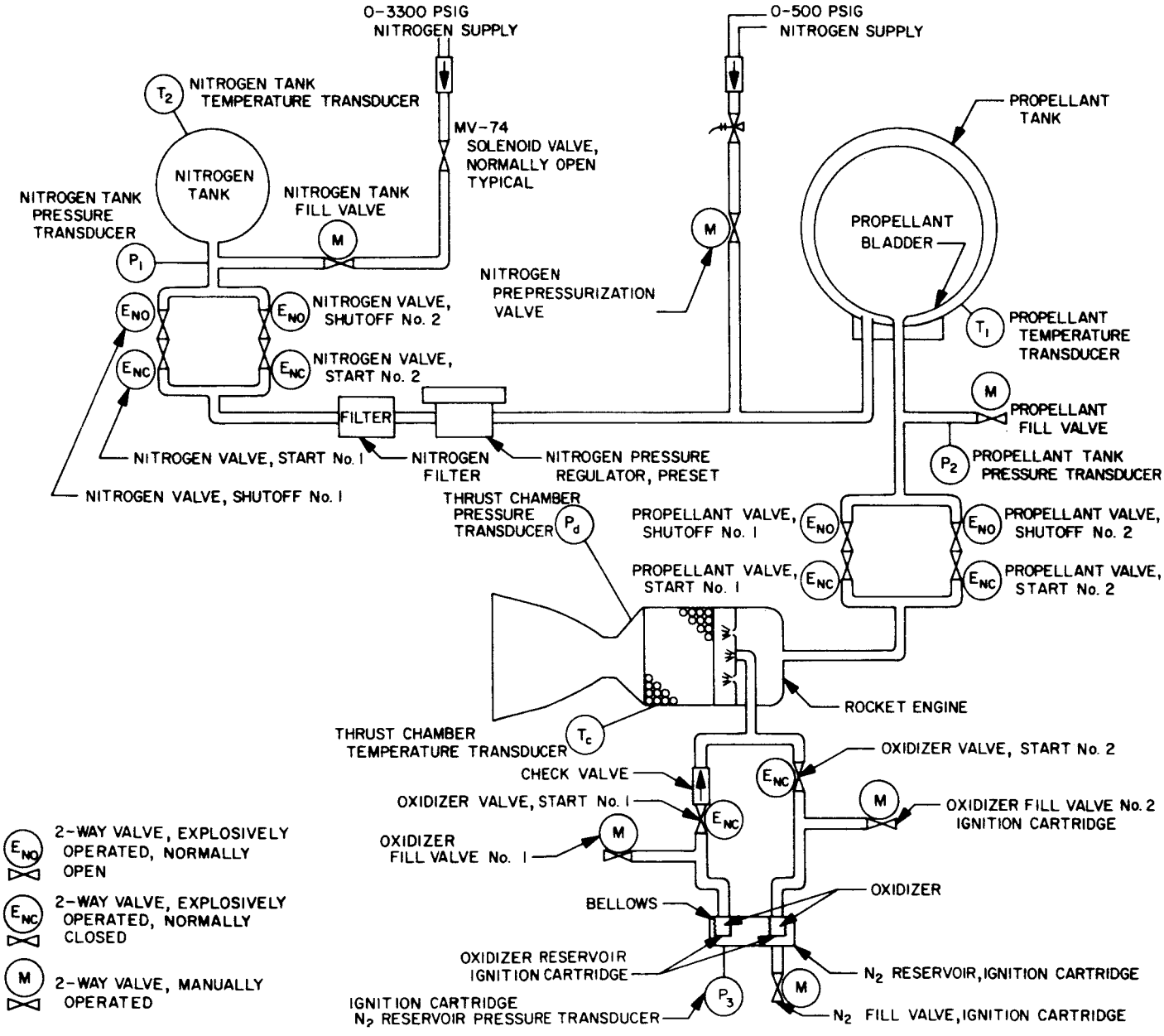

Fig. 21. Test configurations for system firing tests

additional flow tests. Temperature tests are then conducted at 40°F and 131°F. On completion of the temperature tests, the regulator undergoes final flow and lockup tests and is considered ready for system level tests.

5. Explosive Valves

The explosive valves used for flight were from the same lot as those that were subjected to TA testing. Satisfactory completion of the TA tests constituted acceptance of the entire lot of explosive valves; thus, it was not necessary to expend further valves for FA testing.

The flight explosive valves underwent proof and leakage tests. The valves were then subjected to the flight acceptance vibration test. Subsequent to vibration tests, the valves were subjected to final leak tests and were considered ready for flight.

B. System Flight-Acceptance Tests

When component acceptance testing was completed, the rocket engine and pneumatic regulator were assembled in a standard test system, consisting of flight-type hardware—except that a solenoid valve was used in place of the nitrogen explosive valves. The assembled system was subjected to two calibration firings in a vacuum test facility. The first test was 60-sec and the second was 30-sec; during each, data on system performance, total impulse, and general operation were obtained. These data provide thrust-calibration information for subsequent prediction of the engine thrust during the mission.

After completion of the calibration firing, the system was completely assembled for flight. During this process all joints were leak-checked: All liquid seals were leak-checked by filling with gaseous nitrogen under pressure, and all gas seals (nitrogen) were leak-checked by pressurizing with gaseous helium. A mass spectrometer was used to verify the integrity of the high-pressure nitrogen system weldment. For the fill-valve assemblies, a plastic hose was attached to the fill port, the end of the hose was immersed in alcohol, and the meniscus was observed for movement during a 3-min period. All other seals were tested with a soap solution. [10]

[10]Snoop, a product of Nuclear Products Corp., Cleveland, Ohio.

VI. FLIGHT OPERATIONS

A. Mariner III

Mariner III was launched on November 5, 1964. Although the flight of *Mariner III* did not fulfill the mission objectives, it was apparent from telemetry data that the post-injection propulsion system survived the boost environment and remained leak-tight during the period that telemetry was available (7 hr).

The *Mariner III* propulsion system, installed in the spacecraft, was shipped from Pasadena to the Air Force Eastern Test Range (AFETR) by motor van. After an arrival-inspection of the entire spacecraft, the propulsion unit was removed from the spacecraft and subjected to a complete visual inspection and a leak-test. No problems were encountered and the unit was returned to the spacecraft for a final spacecraft system-test sequence. The propulsion system was partially pressurized so that transducers and the telemetry system could be checked out during the spacecraft testing. Several days later, the unit was returned to the propulsion facility for final preparation, fueling, and pressurization, an operation similar to the *Ranger* AFETR procedure discussed in Ref. 2. Loading and pressurization operations of the system proceeded without incident. The pressures in the tankage were monitored for approximately two weeks to assure that no leakage was occurring.

After verifying that the unit was pressure tight, the system was installed in the spacecraft. During the countdown, the readiness of the system was verified by monitoring the pressures and temperatures of the nitrogen tank, oxidizer reservoir, and the fuel tank.

The launch phase was nominal, and telementry data indicated that the propulsion system survived the boost environment. However, at separation + 17 min, the expected microswitch indication of solar panel deployment did not occur. It was decided that the aerodynamic shroud did not jettison, and several commands were sent to the spacecraft in an attempt to verify this condition. A decision was made to undertake a motor-burn in hopes that the resultant spin-up from the off-center thrust might possibly eject the shroud. Since the solar panels were not deployed, the battery lifetime limit was reached prior to the command being sent for engine-ignition and a maneuver was prevented.

B. Mariner IV

Mariner IV was launched on November 28, 1964. The propulsion system performed normally, and the spacecraft completed its mission successfully. Prelaunch operations were similar to those described for *Mariner III*, above.

Inflight telemetry coverage of the *Mariner IV* post-injection propulsion system was excellent throughout the mission. As depicted in Fig. 22 nitrogen tank pressure remained constant up to the time of the post-injection maneuver, indicating a leak-tight system through boost and during the 7-day pre-correction maneuver coast period. This nominal nitrogen tank pressure would have supported a maximum correction maneuver as limited by the amount of fuel available, and resulted in a maximum predicted velocity increment capability of 86.97 m/sec. The fuel-tank pressure (Fig. 23) and oxidizer cartridge pressure (Fig. 24) remained constant prior to launch and up to the time of the correction maneuver.

Based on the pressure regulator setting and nominal engine performance at the expected jet vane deflection, an engine vacuum thrust of 49.40 lbf was predicted. This thrust level, along with the velocity increment requirement of 16.70 m/sec and a spacecraft weight of 574.74 lbm, resulted in a predicted motor burn time of 20.06 sec.

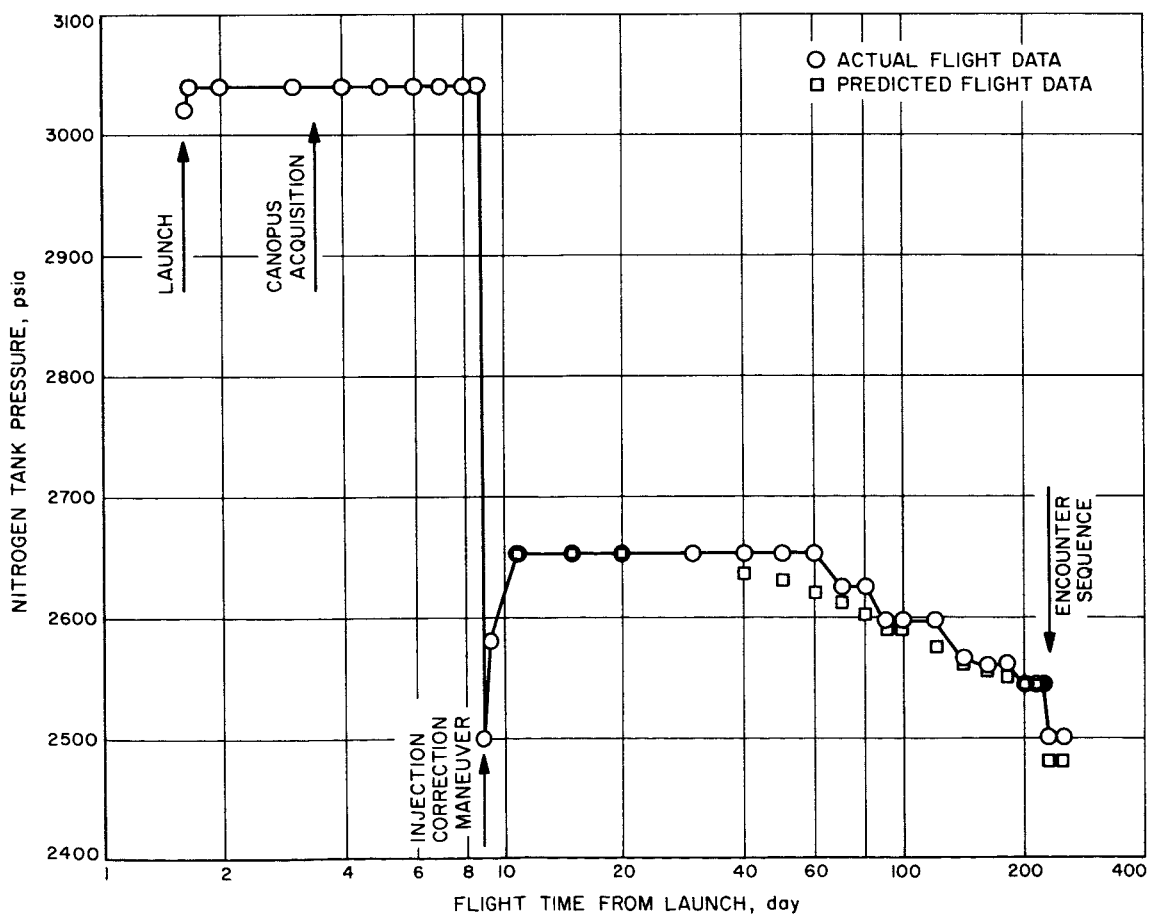

Fig. 22. *Mariner IV* nitrogen tank pressure as a function of flight time

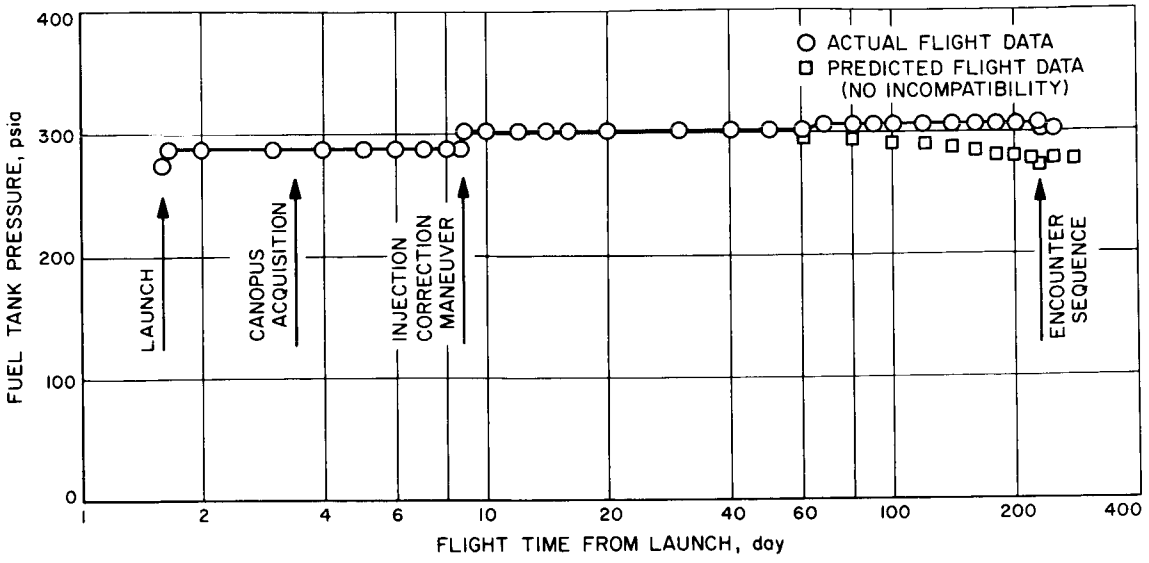

Fig. 23. *Mariner IV* fuel tank pressure as a function of flight time

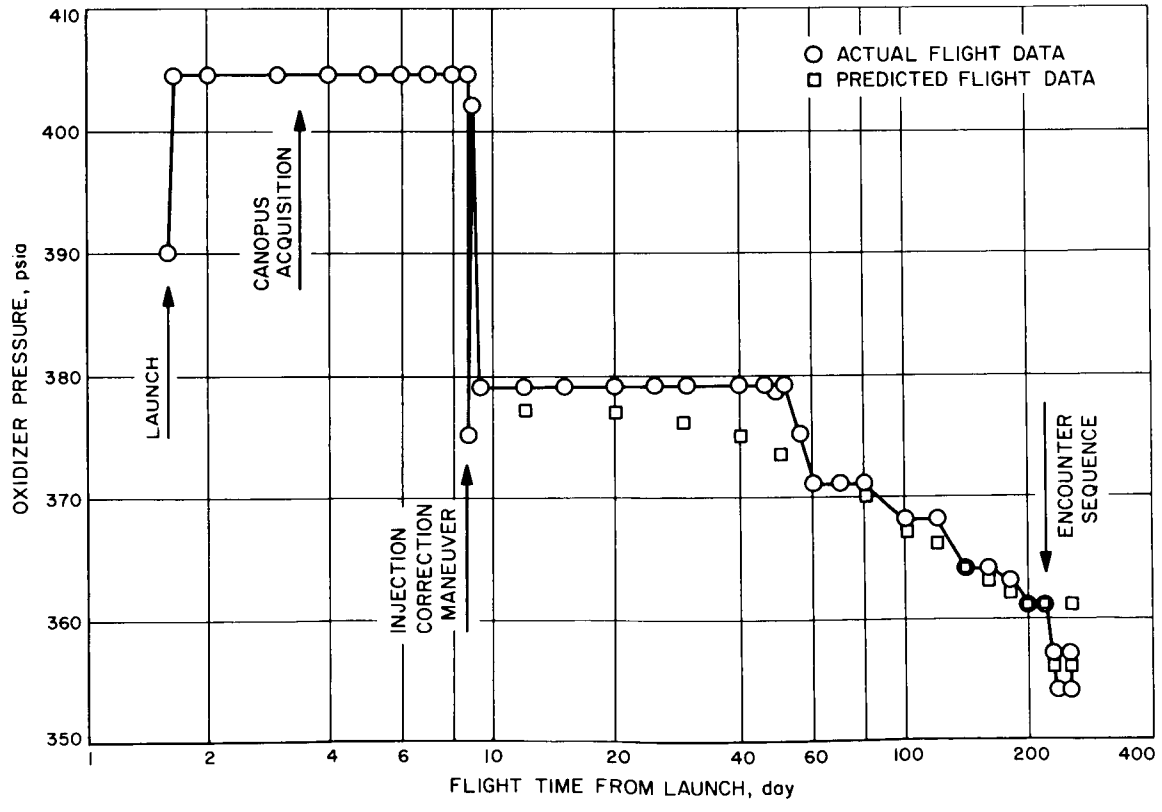

Fig. 24. *Mariner IV* oxidizer pressure as a function of flight time

From the radio signal (Doppler shift) data acquired during the correction maneuver and from the thrust chamber pressure transducer, motor ignition and thrust termination were verified, the burning time being as commanded. Further verification of normal propulsion system operation during the post-injection maneuver was provided by the post-maneuver propellant tank and nitrogen tank pressures and temperatures. Using these data and premaneuver nitrogen- and propellant-tank pressures and temperatures, the delivered velocity increment was calculated to be within 5% of the commanded maneuver. The discrepancy between the calculated velocity increment and the commanded increment (16.70 m/sec) is well within the accuracy of the computation and did not necessarily indicate an error in the execution of the maneuver. Subsequent tracking data indicated that the velocity increment was within 0.3% of that commanded to the spacecraft.

It is significant to note that, because of the inclusion of a timer shutoff mechanism in the *Mariner C* spacecraft, a stringent total impulse predictability and reproducibility requirement was placed on the post-injection propulsion system. Under this criterion the propulsion system performed well within its design limits. In addition, the propulsion system remained leak tight throughout the entire mission, presenting no anomalous torques to the spacecraft and provided the capability for a second post-injection correction.

C. *Abnormal Conditions*

1. Motor-Burn Period

The rocket motor chamber pressure transducer indicated a slightly higher-than-expected value and the propellant tank pressure transducer indicated a slightly lower-than-expected value. By comparing the propellant tank pressure transducer calibration curve against the TA test history data, non-linearity in the region of operating pressure was apparent. In addition, because of a scheduling problem, the motor chamber pressure transducer had not been pressure calibrated prior to flight. Thus, it was not possible to verify the exact performance of the regulator and engine during flight.

2. Cruise Period

At launch + 66 days, a pressure rise of approximately 4 psi (the limit of telemetry resolution) was noted in the fuel tank (Fig. 21). This rise occurred at a time when all other propulsion-oriented pressures and temperatures were dropping. This event was not totally unexpected; a small amount of bladder/hydrazine incompatibility was expected from past test history. However, in attempting to explain the pressure rise, the following three cases were considered:

Case I	Gas leaking through the closed nitrogen explosive valve and regulator
Case II	Gas that is locked up between the nitrogen explosive valve and the regulator leaking through the regulator
Case III	Pressure rise due to gas evolved from a hydrazine/bladder incompatibility

Cases I and II were examined by calculating the leak rates that would result in the indicated pressure rise; these data were not conclusive since the very low magnitude of the pressures involved was on the threshold of the telemetry resolution.

In support of Case III, several bladder tests were initiated, and the data indicated that bladder/hydrazine incompatibility fitted into the pattern of the actual flight data very well. Since the life test system results were similar to the actual flight conditions, an attempt was made to duplicate the degraded condition of the life test bladder. Under controlled conditions, a sample of bladder material was subjected to the temperature/pressure profile of the life test. At an ambient temperature in excess of 100°F, decomposition of hydrazine, caused by the sample bladder, in turn, caused an appreciable rate of pressure increase in the sample vessel. For temperatures below 100°F, the rate of decomposition fell off sharply.

When the sample was removed from the test vessel, its appearance was physically identical to the life-test bladder. From the evidence of these tests and the actual flight data received, there was no detrimental effect to the propulsion system or the spacecraft during the entire mission.

VII. SUMMARY

During the course of the *Mariner C* post-injection propulsion system development program, very few design inadequacies were encountered and, in general, the design approaches taken proved highly satisfactory.

The performance capabilities of the subject propulsion system were entirely adequate for a trajectory-correction propulsion system. For vehicle velocity increment requirements similar to those of *Mariner* (up to 85 m/sec to a 575 lbm spacecraft), the 50 lbf-thrust monopropellant propulsion system presented in this report represents a reproducible, versatile, and relatively efficient spacecraft propulsion system.

A number of improvements become apparent for future designs. It would be desirable to incorporate a more compatible material in the design of the positive expulsion device. The inclusion of a spontaneous catalyst (Ref. 7) for ignition and the use of a liquid regulator (Ref. 8) would increase the simplicity and, thus, the potential reliability of the system.

APPENDIX A
Error Analysis

I. ERROR SOURCES

The following analysis includes a tabulation of error sources (Table A-1), a development of the equations used to calculate resultant impulse errors, and calculations of impulse errors as a function of burn time (time between valve opening and valve closing, or timed-thrust + delay-time) for a first burn of the post-injection propulsion system, assuming no component or inflight telemetry failures or malfunctions. The system as considered in this analysis is shown schematically in Fig. A-1. It consists of a regulated nitrogen pressurization source, a fuel tank and bladder, a feed system with explosively actuated valves and the injector, and a thrust chamber containing a catalyst pack. Not shown is an oxidizer injector that furnishes oxidizer for a bipropellant start.

Table A-1. Propulsion system error sources

Error source	Relation to burn time	Error distribution	Error magnitude
Timing errors			
Ignition delay	Independent	Normal	0.001 sec
Squib & valve (count twice)	Independent	3σ values	0.004 sec
Timed thrust errors			
Thrust calibration			
Transducer	Proportional	Uniform assumed	0.188 lbf
Recorder	Proportional	Uniform assumed	0.188 lbf
Vacuum chamber correction			
Transducer	Proportional	Uniform assumed	0.01 psi
Recorder	Proportional	Uniform assumed	0.001 psi
$C_f A_t P_{cn}$ errors			
P_{cn} calibration	Proportional	Uniform assumed	
Transducer	Proportional	Uniform assumed	0.75 psi
Recorder	Proportional	Uniform assumed	0.65 psi
Tank pressure			
Transducer (calibration)	Proportional	Uniform assumed	1.25 psi
Recorder (calibration)	Proportional	Uniform assumed	0.88 psi
Spring temperature	Zero after P_f transient	Uniform assumed	1 psi
Drift	Zero after P_f transient	Uniform assumed	3 psi
(Use if P_f is not transient)			
Spacecraft transducer	Zero during P_f transient	Uniform assumed	1.75 psi
Telemetry	Zero during P_f transient	Uniform	12 psi
(Use if P_f is transient)			
Fuel temperature			
Transducer (calibration)	Proportional	Uniform assumed	1.76°F
Recorder (calibration)	Proportional	Uniform assumed	1.8°F
Spacecraft transducer	Proportional	Uniform assumed	1°F
Telemetry	Proportional	Uniform	7.5°F
Tailoff impulse	Independent	Normal	
Drag impulse	Independent	Normal	
Error in flow resistance R_1	Proportional	3σ values	4%
Error in oxidizer mass	Independent	Normal 3σ values	0.005 lbm

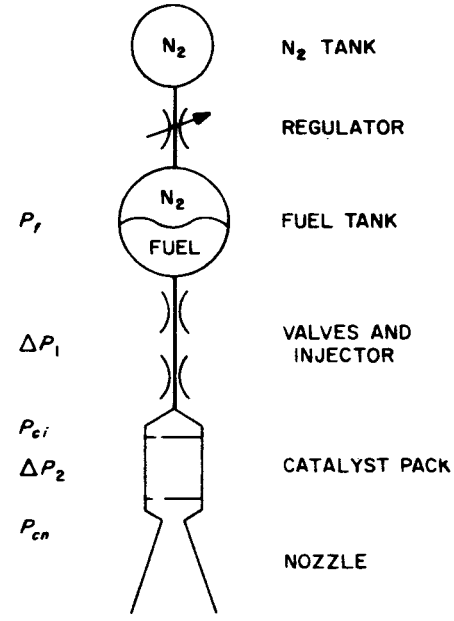

Fig. A-1. System schematic

The thrust sequence is shown in Fig. A-2. The delay time is the time required from squib valve actuation until the pressure in the thrust chamber starts to rise. This includes the time required for the fuel and oxidizer to reach the injector, and the ignition delay. While the oxidizer is being injected, there is a transient in thrust from *zero* to near nominal. If the initial tank-pressure is above or below the regulated pressure, there will be a transient in fuel tank pressure, resulting in an additional thrust transient, as shown. After the fuel shutoff valve closes, there is a tailoff in thrust lasting several seconds. (See Appendix B for a detailed discussion of tailoff impulse.)

Table A-2. Errors independent of burn time

Error	Impulse error calculation
Timing errors	
Ignition delay	0.001 sec × 51 lbf = 0.051 lbf-sec
Squib and valve	0.004 sec × 51 lbf = 0.204 (twice)
Tailoff impulse	0.905
Error in oxidizer mass	0.005 lbm × 214 lbf-sec/lbm = 1.1
	Sum squared = 2.1149
	rss = 1.454 lbf-sec

Numerical values are taken from Tables A-1 and A-7.
Timer errors and CC&S errors are not included.

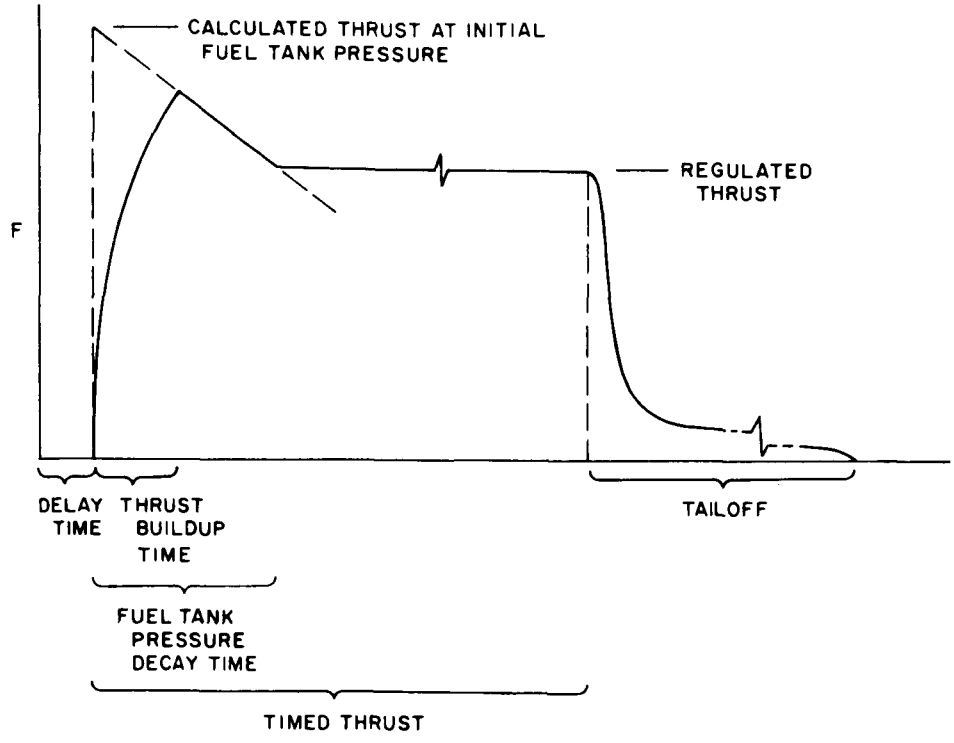

Fig. A-2. General thrust history

Table A-3. Errors proportional to burn time

Error source	Impulse error calculation[a], lbf
After P_f transient	
Timed thrust errors	
Thrust calibration	
Transducer	0.188 lbf × $(3)^{1/2}$ = 0.3256
Recorder	0.188 × $(3)^{1/2}$ = 0.3256
Vacuum chamber correction	
Transducer	0.01 × 6.719 = 0.0672 × $(3)^{1/2}$ = 0.1164
Recorder	0.001 × 6.719 = 0.0067 × $(3)^{1/2}$ = 0.0116
$C_f A_t P_{cn}$ errors	
P_{cn} calibration	
Transducer	0.75 × 0.26811 = 0.2011 × $(3)^{1/2}$ = 0.3483
Recorder	0.65 × 0.26811 = 0.1743 × $(3)^{1/2}$ = 0.3018
Tank pressure	
Transducer (calibration)	1.25 × 0.1209 = 0.1511 × $(3)^{1/2}$ = 0.2617
Recorder (calibration)	0.88 × 0.1209 = 0.1074 × $(3)^{1/2}$ = 0.1860
Spring temperature[b]	1 × 0.1209 = 0.1209 × $(3)^{1/2}$ = 0.2094
Drift[b]	3 × 0.1209 = 0.3627 × $(3)^{1/2}$ = 0.6282
Fuel temperature	
Transducer (calibration)	1.76 × 0.000381 = 0.0007 × $(3)^{1/2}$ = 0.0012
Recorder (calibration)	1.8 × 0.000381 = 0.0007 × $(3)^{1/2}$ = 0.0012
Spacecraft transducer	1 × 0.000381 = 0.0004 × $(3)^{1/2}$ = 0.0007
Telemetry	7.5 × 0.000381 = 0.0029 × $(3)^{1/2}$ = 0.0049
Error in flow resistance R_i	0.04 × 13.22 = 0.5288 × $(3)^{1/2}$ = 0.5288
	Sum squared, without spacecraft transducer and telemetry for tank pressure: 0.82085
	rss: 0.9060
	Sum squared, including spacecraft transducer and telemetry for tank pressure: 1.2593
	rss: 1.1222
During P_f transient	
Timed thrust errors	
$C_f A_t P_{cn}$ errors	
Tank pressure	
Spacecraft transducer	1.75 × 0.1209 = 0.2116 lbf × $(3)^{1/2}$ = 0.3664
Telemetry	12 × 0.1209 = 1.4508 × $(3)^{1/2}$ = 2.513
	Sum squared: 6.449
	rss: 2.539

[a]Numerical values are taken from Tables A-1 and A-7.
[b]Steady-state, only.

The errors can be classified into two groups. First, there are errors independent of burn time, which include: tailoff error, oxidizer start slug mass error, ignition delay error, and valve timing errors. Second, there are errors proportional to burn time which include: errors in thrust prediction—including measurement errors—and the unknown in flow resistance R_1. The jet vane drag error is a nonlinear function of time. If the initial tank pressure P_f is not equal to the regulator output pressure, there will be a transient in P_f which will cause an additional error proportional to the duration of the transient. These groups are tabulated in Tables A-2 and A-3. Errors in the spacecraft timer and the central computer and sequencer (CC&S) are not included in these calculations.

After those errors that are not a function of burn time are converted to impulse, the root sum square (rss) value is calculated. Errors proportional to burn time are first converted to thrust errors and, then, the rss value for these is multiplied by time to obtain an impulse error. The rss value of the combination is next taken. The 3σ values are used for errors that can be approximated as being normally distributed, and the errors that are assumed to be uniformly distributed are multiplied by $\sqrt{3}$ to obtain an effective equivalent of a normally-distributed 3σ error. The transducer errors are assumed to fall into this latter category. The value listed for the tailoff error is based on measurements of very low pressures for several seconds, as discussed in Appendix B. The calculation of tailoff error is shown in Table A-4.

Table A-4. Tailoff error

Low pressure measurement	Calculation			
	Gage size	Error	Impulse Error Constant	Error, lbf-sec
0.35 sec	0 to 300 psia recorder[a]	¾ psi	0.0603 × (3)½ =	0.1045
				0.1045
25 sec	0 to 5 psia recorder	0.05 psi	0.3351 × (3)½ =	0.5804
				0.5804
			Sum squared	0.6957
			rss	0.8341
	Assumed impulse error after end of reading			0.35
			Sum squared	0.8182
			rss	0.9045

[a]For this calculation, recorder errors are assumed to be the same as the instrumentation errors.

The jet-vane drag impulse error is assumed to be 25% of the maximum predicted drag impulse, the integral of the curve in Fig. A-3.

Impulse errors are calculated in this analysis because they are unaffected by changes in estimated spacecraft mass. An example of the velocity increment error is also calculated assuming a spacecraft mass of 570 ±0.5 lbm (3σ); the error is plotted in Fig. A-4. The two cases considered are: (1) nominal start and (2) the system starting with P_f high. The calculations are tabulated in Tables A-5 and A-6.

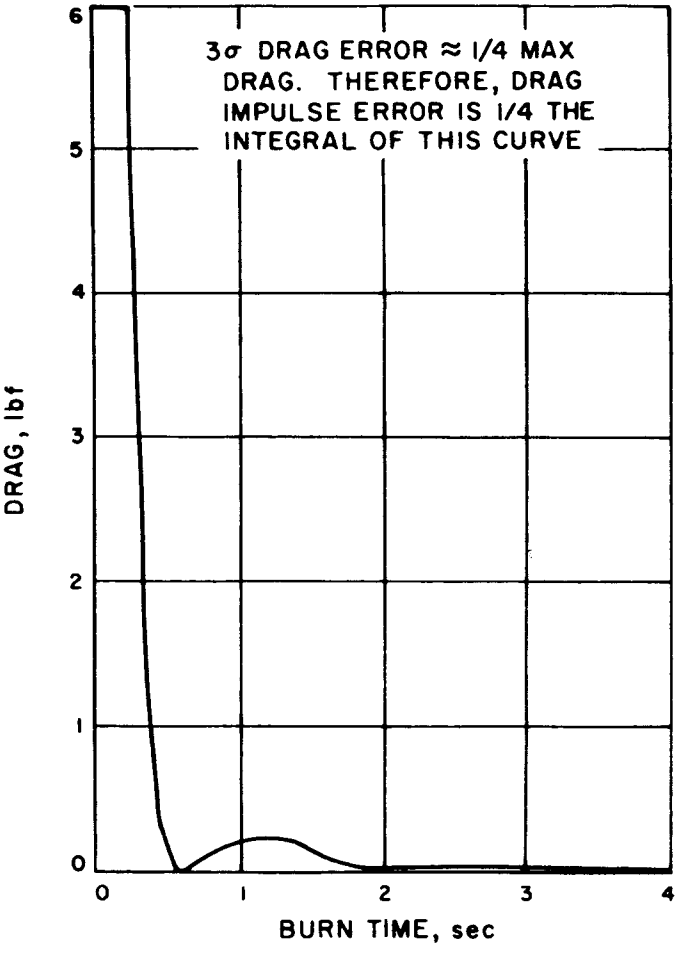

Fig. A-3. Maximum jet vane drag as a function of burning time

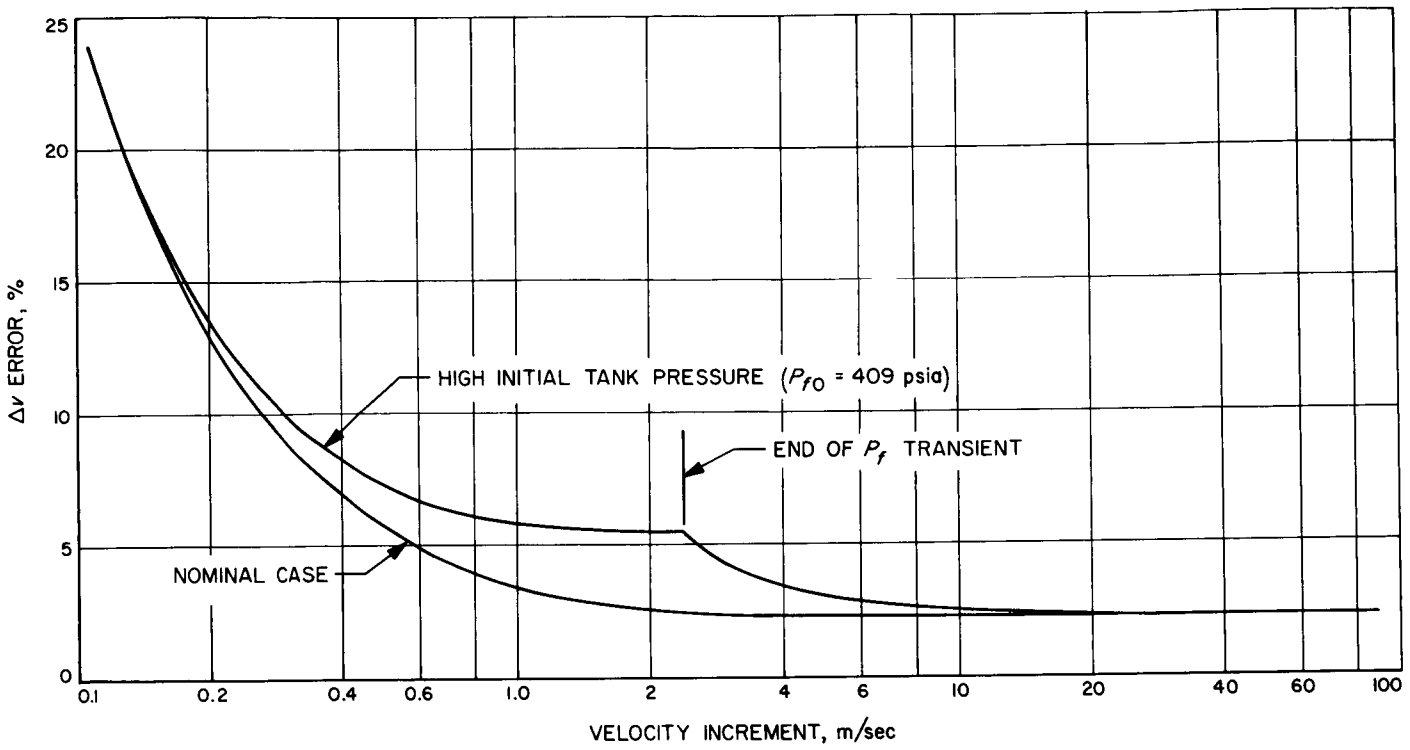

Fig. A-4. 3σ error in velocity increment (%) as a function of velocity increment (570-lb spacecraft)

Table A-5. Calculated errors for nominal start

Burn time, sec	0.075	0.15	0.35	1	5	10	20	100
Impulse	6.15	9.94	20.1	53.0	255	508	1014	5063
Error source	**Resultant impulse error**							
Constant (lbf-sec)	1.454	1.454	1.454	1.454	1.454	1.454	1.454	1.454
Proportional (lbf-sec)	0.0842	0.1683	0.3928	1.122	5.611	11.222	22.44	112.22
Drag (lbf-sec)	0.1125	0.2250	0.47	0.52	0.53	0.53	0.54	0.58
Total (lbf-sec)	1.461	1.481	1.578	1.909	5.821	11.33	22.49	112.23
% Error	23.8	14.9	7.85	3.60	2.28	2.23	2.22	2.22
Change in mass								
Propellant used, lbm	0.02	0.03	0.08	0.22	1.08	2.2	4.32	21.6
Average mass, lbm	569.99	569.98	569.96	569.89	569.46	568.9	567.84	559.2
Resultant velocity increment error								
Δv, m/sec	0.1058	0.1701	0.3458	0.9120	4.391	8.757	17.51	88.79
Δv error, m/sec[a]	0.0251	0.0253	0.0271	0.0329	0.100	0.195	0.389	1.969
% Error	23.8	14.9	7.85	3.60	2.28	2.23	2.22	2.22

[a]Includes 0.5 lbm error (0.09%).

Table A-6. Worst-case[a]: high tank pressure

Burn time, sec	0.075	0.15	0.35	1	2.64	10	20	100
Impulse	6.15	9.94	20.1	53	136	508	1014	5063
Error source	**Resultant impulse error**							
Constant	1.454	1.454	1.454	1.454	1.454	1.454	1.454	1.454
Drag	0.1125	0.225	0.47	0.52	0.53	0.53	0.54	0.58
Transient (lbf-sec)	0.1904	0.3809	0.8887	2.539	6.703	6.703	6.703	6.703
Proportional	0.0680	0.1359	0.3171	0.906	2.392	10.651	21.87	111.6
Total	1.472	1.526	1.796	3.107	7.28	12.68	22.93	111.8
% Error	23.9	15.4	8.93	5.86	5.36	2.50	2.26	2.21
	Resultant velocity increment error							
Δv, m/sec[b]	0.1058	0.1701	0.3458	0.9120	2.385	8.757	17.51	88.79
Δv error, m/sec[c]	0.0253	0.0262	0.0309	0.0534	0.128	0.219	0.396	1.96
% Error[b]	23.9	15.4	8.93	5.86	5.36	2.50	2.28	2.21

[a]This case considers the maximum temperature condition under which the system is expected to operate. System temperature is 125°F, initial tank pressure is 409 psia, initial ullage is 80 in.^{3}, and the tank pressure decay time is 2.64 sec.
[b]From Table A-5.
[c]Includes rss of impulse %-error and spacecraft mass error (0.09%), which is negligible in this case.

II. DEVELOPMENT OF ERROR EQUATIONS

In developing the equations used to calculate the effects of individual error sources, Eqs. (A-1) through (A-6) are written to describe each section of the system. These are solved for chamber pressure as a function of those system variables that have been established to be the important error contributors. (See Nomenclature and Table A-7 for typical values.)

$$P_{cn} = P_f - \Delta P_1 - \Delta P_2 \tag{A-1}$$

$$\Delta P_1 = P_f - P_{ci} = R_1 \frac{\dot{w}_f^2}{\rho_f} \tag{A-2}$$

$$\Delta P_2 = P_{ci} - P_{cn} = R_2 \frac{\dot{w}_f^2}{\rho_c} \tag{A-3}$$

$$\dot{w}_f = \frac{KP_{cn}}{(T_c)^{1/2}} \tag{A-4}$$

$$\rho_c = \frac{P_{cn}}{\mathcal{C}\mathcal{R}_c T_c} \tag{A-5}$$

$$F = C_f A_t P_{cn} \tag{A-6}$$

Equations (A-1) through (A-5) combine to yield

$$P_{cn} = \frac{\rho_f T_c}{2R_1 K^2}\left[-K_2 + \left(K_2^2 + \frac{4R_1 K^2 P_f}{\rho_f T_c} \right)^{1/2} \right] \tag{A-7}$$

where

$$K_2 = 1 + \mathcal{C}\mathcal{R}_c R_2 K^2$$

The contributions of these error sources can be found by taking partial derivatives as follows:

$$\sigma P_{cn} = \left[\left(\frac{\partial P_{cn}}{\partial \rho_f}\,\sigma\rho_f\right)^2 + \left(\frac{\partial P_{cn}}{\partial T_c}\,\sigma T_c\right)^2 + \left(\frac{\partial P_{cn}}{\partial R_1}\,\sigma R_1\right)^2 + \left(\frac{\partial P_{cn}}{\partial P_t}\,\sigma P_f\right)^2\right]^{1/2} \quad (8)$$

Also,

$$\sigma\rho_f = K_1\,\sigma T_f \quad (9)$$

$$\sigma T_c = \frac{C_{pf}}{C_{pc}}\,\sigma T_f \quad (10)$$

From combination of Eqs (A-8), (A-9), and (A-10),

$$\sigma P_{cn} = \left\{\left[\left(\frac{\partial P_{cn}}{\partial \rho_f}K_1 + \frac{\partial P_{cn}}{\partial T_c}\frac{C_{pf}}{C_{pc}}\right)\sigma T_f\right]^2 + \left[\frac{\partial P_{cn}}{\partial R_1}\,\sigma R_1\right]^2 + \left[\frac{\partial P_{cn}}{\partial P_f}\,\sigma P_f\right]^2\right\}^{1/2} \quad (11)$$

The derivatives indicated are the following:

$$\frac{\partial P_{cn}}{\partial \rho_f} = \frac{1}{\rho_f}\left[P_{cn} - \frac{P_f}{\left(K_2^2 + \dfrac{4R_1K^2P_f}{\rho_f T_c}\right)^{1/2}}\right] \quad (12)$$

$$\frac{\partial P_{cn}}{\partial T_c} = \frac{1}{T_c}\left[P_{cn} - \frac{P_f}{\left(K_2^2 + \dfrac{4R_1K^2P_f}{\rho_f T_c}\right)^{1/2}}\right] \quad (13)$$

$$\frac{\partial P_{cn}}{\partial R_1} = -\frac{1}{R_1}\left[P_{cn} - \frac{P_t}{\left(K_2^2 + \dfrac{4R_1K^2P_f}{\rho_f T_c}\right)^{1/2}}\right] \quad (14)$$

$$\frac{\partial P_{cn}}{\partial P_f} = \frac{1}{\left(K_2^2 + \dfrac{4R_1K^2P_f}{\rho_f T_c}\right)^{1/2}} \quad (15)$$

If we let

$$Q_1 \equiv \left(K_2^2 + \frac{4R_1K^2P_f}{\rho_f T_c}\right)^{1/2}$$

and

$$Q_2 \equiv P_{cn} - \frac{P_f}{Q_1}$$

$$\sigma P_{cn} = \left\{\left[Q_2\left(\frac{K_1}{\rho_f} + \frac{1}{T_c}\frac{C_{pf}}{C_{pc}}\right)\sigma T_f\right]^2 - \left[Q_2\frac{\sigma R_1}{R_1}\right]^2 + \left[\frac{\sigma P_f}{Q_1}\right]^2\right\}^{1/2} \quad (16)$$

Table A-7. Nominal values

Symbol	Equivalent	Symbol	Equivalent
A_t (Hot)	0.1527 in.^{2}	T_f	70°F
C	0.03613	V_0	80 in.^{3}
C_f	1.7558	w_f	0.216 lbm/sec
C_{pc}	0.70	$\frac{\partial P_{cn}}{\partial P_f}$	0.4511
C_{pf}	0.73		
F	50.7 lbf		
K^2	0.002942	$R_1 \frac{\partial P_{cn}}{\partial R_1}$	(−) 49.3
K_1	−0.000459		
K_2	1.0529	$\frac{\partial P_{cn}}{\partial T_f}$	(−) 0.00142
P_{cn}	189.1 psia		
P_f	310 psia	$\frac{dF}{dP_f}$	0.1209
Q_1	2.2167		
Q_2	49.3	$R_1 \frac{dF}{dR_1}$	(−) 13.22
R_c	1545 in lbf/lbm°R		
R_1	2380	$\frac{dF}{dT_f}$	(−) 0.000381
R_2	0.3221		
ρ_f	1.0096	$\frac{dF}{dP_0}$	6.72
T_c	2260°R		

If it is assumed that the product $C_f A_t$ is constant, and Eq. (A-6) is differentiated,

$$\sigma F = C_f A_t \, \sigma P_{cn} \tag{17}$$

Errors are then calculated by Eqs. (16) and (17).

A. Fuel Tank Pressure Decay Time

If the system is fired when the fuel tank pressure is above the regulator outlet pressure (Fig. A-1), a finite time will be required for the tank pressure to decay to the regulator pressure. If isentropic expansion and constant fuel flow (average flow during transient) are assumed, we have:

$$V_f = V_0 + V_f \cdot t \tag{18}$$

and

$$P_f (V_0 + V_f \cdot t)^\gamma = P_{f0} V_0^\gamma \tag{19}$$

which, together, form an equation for decay time:

$$t_d = \frac{V_0}{\dot{V}_f}\left[\left(\frac{P_{f0}}{P_f}\right)^{1/\gamma} - 1\right] \tag{20}$$

B. Velocity Increment

Nominal burning time is shown by

$$t\,(\text{sec}) = \frac{M \, \Delta v}{F} \tag{21}$$

It is assumed that the catalyst temperature is constant during tailoff and that all gases are heated or cooled to this temperature.

C. Errors and Unknown Effects

In addition to the obvious error sources in this analysis, such as variations in dimensions and temperature, there are some rather significant unknown quantities. The fuel and oxidizer entering the thrust chamber during tailoff are assumed to react at a constant mixture ratio which gives a maximum impulse because of the bipropellant reaction. This assumption could be in error, and the quantities of propellants assumed to be reacting may not be correct. Since the analysis is *trimmed* to match the data, it is felt that the final calculated numbers for tailoff impulse are accurate to about ±15%. This is based on an error analysis of the system.

II. CALCULATIONS

A. Gas in Chamber

During the bipropellant start, the average temperature of the gas in the thrust chamber is assumed to be the catalyst pack temperature (Fig. B-2). It is assumed that chamber pressure (P_c) is constant until the fuel is shut off. The effective gas volume of the catalyst is calculated by multiplying the catalyst volume by the porosity.

During monopropellant operation, it is assumed that the gas between the injector and the catalyst is cool (800°R) because of the injector spray and because the rest of the gas in the chamber is at the catalyst temperature. However, the specific impulse for all gas is calculated at the catalyst temperature.

Using the perfect gas law to calculate the mass of gas in the chamber, such that $m \sim 1/T_c$, and noting that $I_s \sim \sqrt{T_c}$, it is observed that the impulse due to this gas is inversely proportional to $\sqrt{T_c}$. The mass proportionality is not applied to the gas between the injector and the catalyst after bipropellant ignition because this gas is considered to be cooled to a constant temperature of about 800°R by the spray. This produces a constant term as shown. The mass of this gas is found to be approximately

$$m = \frac{2.98}{T_c}$$

during oxidizer injection, and

$$m = 0.00136 + \frac{1.89}{T_c}$$

after oxidizer injection.

B. Spray Volume

The pressure drop of the injector (ΔP), the flow rate ($\dot{w}$), and the fuel density (ρ) are used to calculate the flow area of the spray, assuming no flow losses in the injector. This value is multiplied by the distance from the injector to the catalyst (L) to obtain an approximate spray volume (V). It is assumed that the fuel is not heated until it reaches the catalyst.

$$V = A \cdot L = \frac{\dot{w} L}{2g\rho\Delta P} = \frac{0.216 \times 0.9}{\left(2 \times 386 \times \frac{1.01 \times 62.4}{1728} \times 100\right)^{1/2}}$$

$$= 0.00423 \text{ in}^3.$$

$$\text{mass} = \rho V = 0.000154 \text{ lbm}$$

Any droplets of the spray that recirculate or bounce around above the catalyst are included in the fuel wetting the catalyst.

C. Fuel Wetting Catalyst

It is known that the injector end of the catalyst bed is wetted by some liquid fuel, but the exact amount is unknown. The maximum wetted depth indicated in Ref. 9 is about 0.52 in. Since the spray hits the catalyst only in small areas, it is assumed that the average wetted depth is about 40% of this, or about 0.2 in. It is further assumed that about half of the volume wetting the catalyst is vapor or gas. Since the temperature of the fuel in this area is not known, the fuel tank temperature is assumed. The volume of fuel is, then, on the order of

$$V = \frac{\pi}{4} D^2 \times 0.52 \times \text{porosity} \times 0.4 \times 0.5, \text{ where } D \text{ is chamber diameter}$$

$$= \frac{\pi}{4}(2.6)^2 \times 0.52 \times 0.335 \times 0.4 \times 0.5$$

$$= 0.185 \text{ in}^3.$$

Since this number is only a rough approximation, it is adjusted to match the calculations to the data. The number that best correlates with the data is 0.124 in.^{3}

D. Oxidizer

The oxidizer is assumed to vaporize, then react with both the fuel wetting the catalyst in the chamber and the fuel trapped in the injector manifold as it vaporizes into the chamber. The mixture ratio is calculated as the total oxidizer that remains in the lines divided by the sum of the fuel in the injector and the fuel in the chamber. The gas is then assumed to exit at the catalyst bed temperature. It is assumed that during the bipropellant start period there is no fuel wetting the catalyst.

The initial mass of oxidizer for each burn is 0.06 lbm and the trapped volume after the oxidizer injection (0.84 sec) is 0.159 in.^{3} for the first burn and 0.132 in.^{3} for the second burn. Constant oxidizer flow is assumed during the injection. The resultant impulse is plotted in Fig. B-3.

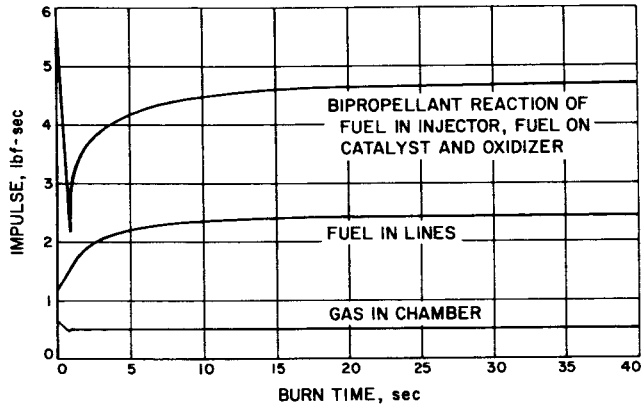

Fig. B-3. *Mariner* C components of calculated tailoff impulse

E. Fuel

The fuel specific impulse (I_s) is based on a nominal value of 235 lbf-sec/lbm. Reference 9 shows that the degree of dissociation of the fuel is very nearly independent of flow rate and chamber pressure for this case. Therefore, the ratio of specific heats and the molecular weight will be nearly constant, so it is assumed that the thrust coefficient and characteristic exhaust velocity are functions of temperature, only, for the monopropellant.

The specific impulse is, then:

$$I_s = 4.892\,(T_c)^{1/2}$$

F. Volumes

Volumes of the fuel and oxidizer trapped in the lines are calculated by adding the volumes of each section of the lines and the injector. These are not exactly the same for the second burn as for the first. They are:

	1st burn vol, in.^{3}	2nd burn vol, in.^{3}
Fuel in lines	0.289	0.317
Fuel in injector	0.230	0.230
Oxidizer	0.159	0.132

G. Temperature Effects

Changes in temperature (T) of the system could change the tailoff impulse (I_t) by a percent or two. A plot of $\partial I_t/\partial T$ is shown in Fig. B-4. In calculating this curve it is assumed that $\partial I_c/\partial T = C_{pf}/C_{pc}$, where T_c is the stagnation gas temperature, C_{pf} is the specific heat of the fuel, and C_{pc} is the specific heat of the chamber gases. The function shown on the figure is time dependent because the specific

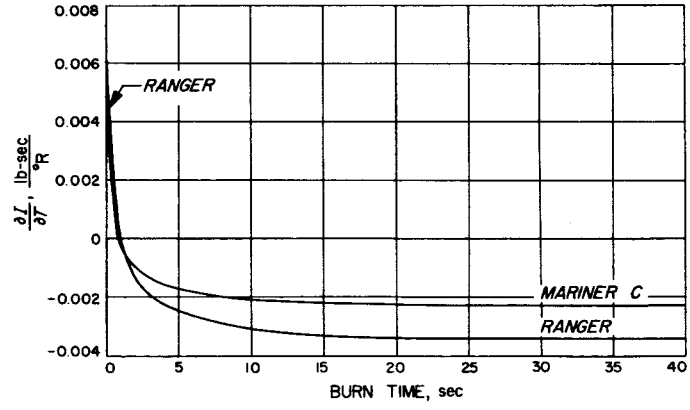

Fig. B-4. Calculated change in tailoff impulse with respect to system temperature as a function of burning time

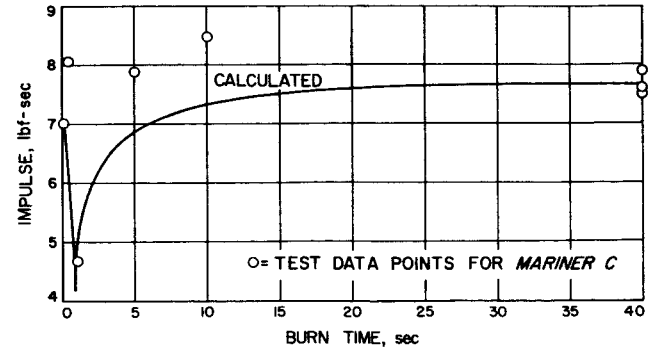

Fig. B-5. *Mariner* C calculated tailoff impulse and test data points as a function of time

impulse varies with T_c, which is a function of time. Comparison of Figs. B-4 and B-5 show that the maximum tailoff impulse change due to temperature uncertainty is about 0.05%/°F. This is negligible if temperature of the system at the time of ignition is known to within ±10°F. Data points shown in Fig. B-5 are corrected to 70°F. Table B-1 contains a tabulation of these data and the corrections.

Table B-1. *Mariner C* tailoff impulse test data

Run	Temp, °F	Time, sec	I, lbf-sec	$\Delta I/\Delta T$, lbf-sec/°F	ΔI, lbf-sec	Modified I, lbf-sec	Burn
95	69	60	7.90	−0.00231	−0.002	7.90	1st
96	66	0.1	7.01	0.00410	0.016	7.03	2nd
98	86	60	7.43	−0.00231	0.037	7.47	1st
99	80	0.3	8.11	0.00291	−0.029	8.08	2nd
101	102	60	7.48	−0.00231	0.074	7.55	1st
102	99	1	4.60	−0.00017	0.005	4.60	2nd
103	95	5	7.78	−0.00170	0.043	7.82	1st
104	92	10	8.39	−0.00207	0.046	8.44	2nd

H. Thrust Chamber Cooling

Test results show that the catalyst bed is not appreciably cooled during tailoff. It is surmised that cooling due to radiation and conduction is offset by the heat generated from the bipropellant reaction and the monopropellant decomposition during tailoff.

The temperature curve used for this analysis is shown in Fig. B-2. It is taken directly from test results and is considered typical.

III. CONCLUSIONS

The calculated curve in Fig. B-5 and the test data points for *Mariner C* correlate very well (note plotted experimental points). The curve was based entirely on calculated volumes and performance, with one exception—the volume of fuel wetting the catalyst. This parameter was adusted 33% to obtain the best match to the experimental data for the long burn times. It is believed that these tailoff impulse calculations are accurate to within ±15%.

NOMENCLATURE

Appendixes A and B

A_e Nozzle exit area

A_t Throat area

$\mathscr{C}$ Constant in ρ_c equation

C_f Thrust coefficient

C_{pc} Specific heat of thrust chamber gas

C_{pf} Specific heat of fuel

F Thrust

I_D Drag impulse

I_s Specific impulse

K Constants

M Spacecraft mass

P_{ci} Thrust chamber pressure, injector end

P_{cn} Thrust chamber pressure, nozzle end

P_f Fuel tank pressure

Q Lumped parameter

$\mathscr{R}_c$ Gas constant for chamber gases

$R_{1,2}$ Fluid resistance factors

t_d Delay time

T_c Thrust chamber temperature

T_f Fuel temperature

v Velocity

V_0 Initial fuel tank ullage volume

V_f Fuel tank ullage volume

ε Nozzle area ratio

γ Ratio of specific heats of pressurizing gas

ρ_c Specific gravity of thrust chamber gas

ρ_f Specific gravity of fuel

w_f Fuel flow rate

REFERENCES

1. Propulsion Sections, *Mariner C* Project Reports, *Space Programs Summary, Nos. 37-19—37-24; No. 37-26, No. 37-27,* and *No. 31, Volume II,* Jet Propulsion Laboratory, Pasadena, California, January 31, 1963 through January 31, 1965. (Confidential)

2. Evans, D. D., Groudle, T. A., Mattson, R. F., *Development of the Ranger Block-III Spacecraft Propulsion System,* Report No. 32-829, Jet Propulsion Laboratory, Pasadena, California, February 1, 1965.

3. *Space Programs Summary, No. 37-26, Volume II,* Jet Propulsion Laboratory, Pasadena, California, March 31, 1964. pp. 42–47. (Confidential)

4. "Procedures in Sensitivity Experiments," Report No. 101. IRSRG-P, Statistical Research Group, Princeton University, May 1944.

5. Macglashan, W. F., Jr., *Fill Valve Development for the Advanced Liquid Propulsion System (ALPS),* Report No. 32-875, Jet Propulsion Laboratory, Pasadena, California, February 1, 1966.

6. "Bladder Materials Investigation," *Space Programs Summary, No. 37-32, Volume II,* Jet Propulsion Laboratory, Pasadena, California, March 31, 1965. p. 29. (Confidential)

7. *Development of Spontaneous Catalyst for the Thermal Decomposition of Hydrazine,* Report No. S-13889, Shell Development Co., Emeryville, California, June 1963. (Confidential)

8. Porter, R. N., Evans, D. D., "Advanced Propulsion System for Unmanned Spacecraft," *Astronautics and Aeronautics,* Vol. 3, No. 6, June 1965. pp. . . .

9. Grant, A. F., Jr., *Basic Factors Involved in the Design and Operations of Catalytic Monopropellant Hydrazine Reaction Chambers,* Report No. 20-77, Jet Propulsion Laboratory, Pasadena, California, December 31, 1954. (Confidential)